



Suppression of tumor growth by intratumoral injection of short hairpin RNA-expressing plasmid DNA targeting β -catenin or hypoxia-inducible factor 1 α

Yuki Takahashi, Makiya Nishikawa, Yoshinobu Takakura *

Graduate School of Pharmaceutical Sciences, Kyoto University, Kyoto, Japan

Department of Biopharmaceutics and Drug Metabolism, Graduate School of Pharmaceutical Sciences, Kyoto University, Sakyo-ku, Kyoto, 606-8501, Japan

Received 25 July 2006; accepted 8 September 2006

Available online 16 September 2006

Abstract

To inhibit the growth of murine melanoma B16 cells in mice, we downregulated the gene expression of β -catenin and hypoxia-inducible factor 1 α (HIF1 α) in the tumor cells by delivering short hairpin RNA (shRNA)-expressing plasmid DNA (pDNA) targeting one of these genes. Transfection of any of the shRNA-expressing pDNAs to B16 cells resulted in the reduction of the corresponding mRNA, which was associated with a reduced number of viable cells. A flow cytometric analysis of annexin V labeling assay was also performed to count the number of apoptotic cells. A flow cytometric analysis showed that the suppression of the expression of β -catenin or HIF1 α in B16 cells increased the number of apoptotic cells. An intratumoral injection of psh β -catenin (shRNA-expressing pDNA targeting β -catenin) or pshHIF1 α (shRNA-expressing pDNA targeting HIF1 α) followed by electroporation greatly suppressed the expression of the corresponding target mRNA in the intradermal tumor tissue. The growth of the intradermal tumor was significantly ($P < 0.05$) suppressed by the treatment. In conclusion, tumor growth was successfully inhibited by the intratumoral delivery of psh β -catenin or pshHIF1 α .

© 2006 Elsevier B.V. All rights reserved.

Keywords: RNAi; Gene delivery; In vivo; Primary tumor; Electroporation

1. Introduction

Tumor cells are characterized by changes in the profile of protein expression. Such changes may lead to the imbalanced production of proteins relating to the malignancy of the cells, or to the production of mutated proteins with abnormal functions. The altered protein expression in tumor cells may contribute to the cell survival, unregulated proliferation and metastatic nature of the cells. Therefore, silencing the expression of these proteins in tumor cells can be a potent and target-specific cancer treatment with a low risk of side effects. RNA interference (RNAi) is a potent and ubiquitous gene silencing mechanism that downregulates the expression of a specific gene of interest [1–5]. After the discovery that short double-stranded RNA (siRNA) can induce RNAi in mammalian cells without

stimulating interferon response [6,7], siRNAs have proven to be effective agents for suppressing specific gene expression. The early successes of induction of RNAi in cultured cells have led to high expectations for in vivo and therapeutic applications of siRNAs [8,9]. Cancer is one of the most important target diseases for RNAi-based treatment [10,11]. Contrary to conventional strategies, such as the use of antisense oligonucleotides which have been hampered by low potency and insufficient specificity, the use of siRNAs is reported to be more efficient and to have greater in vivo potency [12–15]. Therefore, RNAi-based gene silencing is a promising approach to achieve target-specific anticancer treatments.

Delivery of siRNA to tumor cells is the greatest obstacle to establishing RNAi as a therapeutic approach to treat cancer because the gene silencing effect is limited to cells that have received siRNA [16–18]. This is a major reason why few papers have reported the successful suppression of in vivo tumor growth by RNAi. In a previous study, we have investigated the

* Corresponding author. Tel.: +81 75 753 4615; fax: +81 75 753 4614.

E-mail address: takakura@pharm.kyoto-u.ac.jp (Y. Takakura).

delivery of siRNA or short hairpin RNA (shRNA)-expressing plasmid DNA (pDNA) to tumor cells in mice [19]. We succeeded in effectively suppressing target gene expression in tumor cells by intratumoral injection of siRNA or shRNA-expressing pDNA followed by electroporation. Using melanoma cells stably expressing firefly luciferase, we found that a single intratumoral injection of shRNA-expressing pDNA following electroporation inhibits the expression by 30%. These results suggest that the delivery of shRNA-expressing pDNA can inhibit the tumor growth if a proper target gene in tumor cells is downregulated by this technique.

In addition to the delivery methods of siRNA, selection of target genes is an important issue that determines the RNAi effects on tumor growth. Although many genes encoding products that play important roles in tumor progression can be targets for RNAi-based suppression of tumor growth, we selected β -catenin and hypoxia-inducible factor 1 α (HIF1 α) genes as possible target genes to realize RNAi-based cancer therapy. β -catenin plays a key role in cell adhesion and also regulates the activity of certain transcription factors, T cell factor/lymphoid enhancer factor (TCF/LEF) in the Wnt pathway, which activates the transcription of genes related to cell growth and survival [20]. When injected intraperitoneally, siRNA targeting β -catenin complexed with Oligofectamine suppressed the proliferation of colon cancer HCT116 cells in the peritoneal cavity [21]. On the other hand, HIF1 is a heterodimer that consists of constitutively expressed HIF1 β and HIF1 α , and the expression of the latter is tightly regulated by oxygen concentration. HIF1 activates the transcription of genes that are involved in cancer biology, including angiogenesis, cell survival, glucose metabolism and invasion [22]. Sun et al. reported that intratumoral administration of pDNA which expresses antisense HIF1 suppressed the growth of tumor tissue [23]. In addition, HIF1 was evaluated as a cancer therapeutic target via inducible RNA interference in vivo [24].

Therefore, suppressing the expression of these target genes is expected to inhibit tumor growth. To suppress the expression of these target genes, we constructed and used shRNA-expressing pDNA, not siRNA, to induce RNAi in tumor cells, because (i) shRNA-expressing pDNA shows more sustained RNAi effects than siRNA, and (ii) there was little difference in the delivery efficiency to tumor cells between shRNA-expressing pDNA and siRNA. We report here that shRNA-expressing pDNA targeting β -catenin or HIF1 α effectively suppresses tumor growth in mice following intratumoral injection followed by electroporation.

2. Materials and methods

2.1. shRNA-expressing pDNA

shRNA-expressing pDNAs driven by human U6 promoter were constructed from piGENE-hU6 vector (iGENE Therapeutics, Tsukuba, Japan) according to the manufacturer's instructions. Target sites in murine genes encoding β -catenin and HIF1 α were as follows: β -catenin site1, 5'-GCGGTAGGG TAAATCAGTA-3', site2, 5'-GAATGAGACTGCAGATCTT-3'; HIF1 α site1, 5'-GTGAAAGGATTCATATCTA-3', site2, 5'-

GACACAGCCTCGATATGAA-3'. These pDNAs transcribe a stem-loop-type RNA with loop sequences of ACG UGU GCU GUC CGU. piGENE-hU6 vector, which transcribes a non-related sequence of RNA with partial duplex formation, was used as a control pDNA throughout the present study. Each pDNA was amplified in the DH5 α strain of *Escherichia coli* and purified using a QIAGEN Endofree Plasmid Giga Kit (QIAGEN GmbH, Hilden, Germany).

2.2. Cell culture

A murine melanoma cell line B16-F1, B16-BL6 and B16-BL6 cells that stably express firefly luciferase and sea pansy luciferase (B16-BL6/dual Luc) were cultured in Dulbecco's modified Eagle's minimum essential medium (DMEM; Nissui Pharmaceutical, Tokyo, Japan) supplemented with 10% fetal bovine serum (FBS) and penicillin/streptomycin/L-glutamine (PSG) at 37 °C and 5% CO₂/95% air [19].

2.3. In vitro transfection

B16 cells were plated on culture plates. After an overnight incubation in DMEM containing 10% FBS and PSG at 37 °C in 5% CO₂/95% air, transfection of pDNA was performed using Lipofectamine 2000 (Invitrogen, Carlsbad, CA, USA) according to the manufacturer's instructions. In brief, 1 μ g pDNA was mixed with 3 μ g Lipofectamine 2000 at a final concentration of 2 μ g pDNA/ml dissolved in OPTI-MEM I (Invitrogen), and the resulting complex was added to the cells and the cells were incubated with the complex for 4 h. Cells were washed with PBS and further incubated with the culture medium as described above for specified time periods up to 96 h.

2.4. mRNA quantification

Total RNA was isolated using MagExtractor MFX-2100 and a MagExtractor RNA kit (TOYOBO, Osaka, Japan) following the manufacturer's protocol. To eliminate DNA contamination, the total RNA was treated with DNase I (Takara Bio, Otsu, Japan) prior to reverse transcription. Reverse transcription was performed using a SuperScript II (Invitrogen) and dT-primer following the manufacturer's protocol. For quantitative mRNA expression analysis, real-time PCR was carried out with total cDNA using a LightCycler instrument (Roche Diagnostics, Basle, Switzerland). The sequences of the primers used for amplification were as follows: GAPDH forward, 5'-CTGCCA AGTATGATGACATCAAGAA-3', reverse, 5'-ACCAGGAAA TGAGCTTGACA-3'; β -catenin forward, 5'-CCTGCAGAAC TCCAGAAAG-3', reverse, 5'-GTGGCAAAAACATCAAC GTG-3'; HIF1 α forward, 5'-TCAAGTCAGCAACGTGGA AG-3', reverse, 5'-TATCGAGGCTGTGTCGACTG-3'. Amplified products were detected on-line via intercalation of the fluorescent dye SYBR green (LightCycler-FastStart DNA Master SYBR Green I kit, Roche Diagnostics). The cycling conditions were as follows: initial enzyme activation at 95 °C for 10 min, followed by 55 cycles at 95 °C for 10 s, 60 °C for 5 s, and 72 °C for 20 s. Gene-specific fluorescence was measured at

72 °C. The mRNA expression of target genes was normalized by using the mRNA level of GAPDH.

2.5. Effect of shRNA-expressing pDNAs on proliferation of B16 cells

B16-BL6/dual Luc cells were transfected with pDNA as described above. After the transfection of pDNAs for 4 h, cells were washed with PBS and further incubated with the culture medium for specified time periods up to 96 h. The cell numbers at the indicated time points were evaluated by MTT assay as described previously [25].

2.6. Flow cytometric determination of apoptosis

B16-BL6/dual Luc cells seeded on 6-well culture plates were treated with pDNA as described above. At 3 days after transfection, adherent cells were detached by trypsinization and re-suspended in PBS. Aliquots of these cell suspensions were centrifuged and the pellets were used for the flow cytometric determination of apoptosis using a commercial kit (Vybrant™ Apoptosis Assay Kit #2, Molecular Probes, Invitrogen). In brief, a cell pellet was re-suspended in a binding buffer (10 mM HEPES, 140 mM NaCl, 2.5 mM CaCl₂, pH 7.4) to give a cell density of approximately $2\text{--}10 \times 10^5/\text{ml}$. Aliquots (100 μl) of this cell suspension were incubated with 5 μl recombinant annexin V labeled with Alexa Fluor® 488 dye (Alexa Fluor 488 annexin V) and 1 μl of a stock solution of propidium iodide (PI, 100 $\mu\text{g}/\text{ml}$) for 15 min at room temperature. After the incubation period, 400 μl of the binding solution was added and the samples were kept on ice until analysis in the flow cytometer. Samples were analyzed on a flow cytometer (FACScan, BD, Franklin Lakes, NJ, USA) and electronic compensation was used to remove spectral overlap. Annexin V staining, DNA signals and side scatter (SSC) signals were detected on a log scale. Forward (FSC) signals were detected in a linear mode. The FL1 and FL2 photomultiplier (PMT) voltage settings were set using unstained isotype samples. The threshold using FSC was set to exclude debris without excluding any populations of interest. The flow cytometric data were analyzed with WINMDI 2.8 software®.

2.7. Animals

Seven-week-old male C57/BL6 mice, purchased from Shizuoka Agricultural Cooperative Association (Shizuoka, Japan) were used in all the experiments. All animal experiments were conducted in accordance with the principles and procedures outlined in the US National Institutes of Health Guide for the Care and Use of Laboratory Animals. The protocols for animal experiments were approved by the Animal Experimentation Committee of Graduate School of Pharmaceutical Sciences of Kyoto University.

2.8. Primary tumor model

B16-BL6 cells in an exponential growth phase were harvested by trypsinization and suspended in Hanks' balanced salt solution

(HBSS, Nissui Pharmaceutical). The tumor cells (2×10^5 cells) were injected intradermally into the back of syngeneic C57/BL6 mice. When the tumor diameter reached 2–3 mm (1 week after tumor inoculation), mice received a single intratumoral injection of 30 μg pDNA dissolved in 50 μl saline at a time followed by twelve electric pulses (1000 V/cm, 5 ms, 4 Hz) which were delivered through a pair of 1-cm² forcep-type electrodes connected to a rectangular direct current generator (CUY21, Nepagene, Chiba, Japan). In the growth inhibition experiment, shRNA-expressing pDNAs were administered at day 7, 10 and 19 after tumor inoculation. Tumor growth was evaluated by measuring the tumor size using calipers at indicated times, and tumor volume (mm³) was calculated from the following equation: (longest diameters \times shortest diameters)^{3/2} \times $\pi/6$.

2.9. Statistical analysis

Differences were statistically evaluated by Student's *t*-test. A *P*-value of less than 0.05 was considered to be statistically significant.

3. Results

3.1. Reduction in mRNA by transfection of shRNA-expressing pDNA to B16-F1 cells

Two candidate sequences were selected for each target gene. Fig. 1 shows the mRNA levels of the target genes in B16-F1 cells 24 h after transfection of shRNA-expressing pDNA targeting β -catenin or HIF1 α measured by real-time RT-PCR. The transfection of shRNA-expressing pDNA maximally suppressed the mRNA expression of β -catenin and HIF1 α to about 20% and 25% of each control value, respectively. For each target gene, an shRNA-expressing pDNA (#2 in all cases)

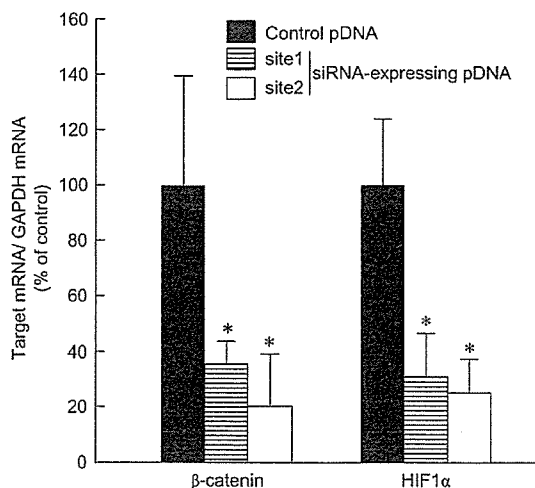


Fig. 1. Reduction of mRNA in B16 cells following transfection of shRNA-expressing pDNA. B16-F1 cells seeded on 12-well culture plates (at a density of 2×10^5 cells/well) were transfected with shRNA-expressing pDNA or piGENE-hU6. Amounts of mRNA were determined 24 h after transfection. The results are expressed as the mean \pm S.D. ($n=3$). **P*<0.05 for Student's *t*-test versus control group.

was selected based on the inhibitory effect, and was used in the subsequent experiments. The selected shRNA-expressing pDNAs were named as psh β -catenin and pshHIF1 α .

3.2. Growth inhibition of B16-BL6/dual Luc cells by shRNA-expressing pDNA

To evaluate the inhibitory effect of shRNA-expressing pDNA on tumor cell growth in vitro, the time course of the number of B16-BL6/dual Luc cells after the transfection of shRNA-expressing pDNAs was measured by MTT assay (Fig. 2). Transfection of psh β -catenin or pshHIF1 α reduced the number of viable B16 cells to about 50% and 60% of the control value, respectively. A significant reduction in the viable cell number was observed in the psh β -catenin- or pshHIF1 α -treated cells as early as 1 and 2 days after transfection, respectively. Therefore, these results indicate that psh β -catenin and pshHIF1 α are potent in inhibiting the proliferation of B16 cells.

3.3. Flow cytometric analysis of cell death induced by shRNA-expressing pDNAs

Flow cytometric analysis of cells stained with fluorescein-labeled annexin V and PI was performed to detect apoptotic and necrotic cells after transfection of shRNA-expressing pDNAs to B16-BL6/dual Luc cells (Fig. 3). At 3 days after transfection of shRNA-expressing pDNA, cells were stained with annexin-FITC and PI. Fig. 3A–C shows the typical results of the flow cytometric analysis of the cells. Live cells (annexin-FITC and PI double negative) occupy the lower left quadrant, early apoptotic cells (annexin-FITC positive and PI negative) occupy the lower right quadrant and late apoptotic or necrotic cells (annexin-FITC and PI double positive) occupy the upper right quadrant. Fig. 3D summarizes the number of viable, early apoptotic, or late apoptotic and necrotic cells. Transfection of psh β -catenin or pshHIF1 α increased the number of apoptotic cells compared with that of control pDNA. The number of dead cells, which

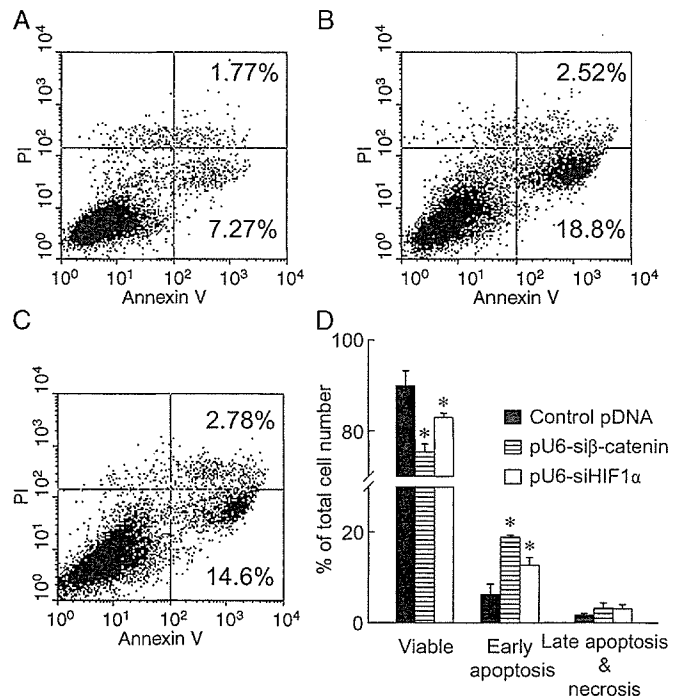


Fig. 3. Induction of apoptosis and necrosis in B16-BL6 cells caused by transfection of shRNA-expressing pDNA. (A–C) Representative dot plots of the flow cytometric quantification of intact, apoptotic and necrotic cells. B16-BL6/dual Luc seeded on 6-well culture plates (at a density of 1×10^5 cells/well) were transfected with piGENE-hU6 (A), psh β -catenin (B) or pshHIF1 α (C). After 3 days incubation from the initiation of transfection, cells were processed and stained with annexin-FITC and PI as indicated in M&M. Live cells (annexin-FITC and PI double negative) occupy the lower left quadrant, early apoptotic cells (annexin-FITC positive and PI negative) occupy the lower right quadrant and late apoptotic or necrotic cells (annexin-FITC and PI double positive) occupy the upper right quadrant. (D) Percentage of viable, early apoptotic and late apoptotic or necrotic cells after transfection of shRNA-expressing pDNA, as calculated from the dot plots as in panel (A–C). The results are expressed as the mean \pm S.D. ($n=3$). * $P < 0.05$ for Student's t -test versus control group.

was roughly estimated as the total number of apoptotic and necrotic cells, was about 20% of the total cells in the case of psh β -catenin, 15% in the case of pshHIF1 α and 10% in the case of control pDNA.

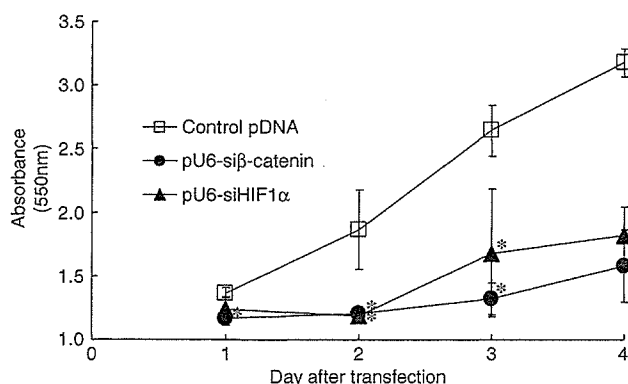


Fig. 2. Anti-proliferative effect of shRNA-expressing pDNA against B16 cells. B16-BL6/dual Luc seeded on 24-well culture plates (at a density of 2×10^4 cells/well) were transfected with shRNA-expressing pDNA or piGENE-hU6. Cell populations at indicated time points were evaluated by MTT Assay. The results are expressed as the mean \pm S.D. ($n=3$). * $P < 0.05$ for Student's t -test versus control group.

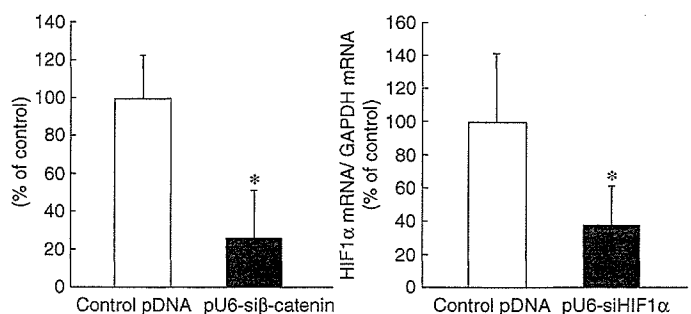


Fig. 4. Reduction of mRNA expression in primary tumor tissue by intratumoral injection of shRNA-expressing pDNA followed by electroporation. Mice received an intratumoral injection of piGENE-hU6 or shRNA-expressing pDNA (30 μ g), followed by electroporation. Amounts of mRNA in tumor tissue were determined 24 h after administration. The results are expressed as the mean \pm S.D. ($n=4$). * $P < 0.05$ for Student's t -test versus control group.

3.4. Reduction of mRNA and growth inhibition of subcutaneous tumor tissue of B16-BL6/dual Luc by intratumoral injection of psh β -catenin or pshHIF1 α

Fig. 4 shows the amount of β -catenin and HIF1 α mRNA in B16 tumor tissue in mice 24 h after intratumoral injection of psh β -catenin or pshHIF1 α followed by electroporation. A single injection of each shRNA-expressing pDNA reduced the amount of the corresponding target mRNA in the tumor tissue. The mRNA level of β -catenin and HIF1 α was reduced to 25 and 35% of the control value, respectively, demonstrating that intratumoral injection of shRNA-expressing pDNA can efficiently suppress the corresponding target gene expression in tumor tissue in mice.

To suppress the tumor growth in mice, tumor-bearing mice received intratumoral injection of shRNA-expressing pDNA followed by electroporation at day 7, 10 and 19 days after tumor inoculation. The injection of control pDNA followed by electroporation retarded the growth of tumor tissue compared with the no treatment group (data not shown). Intratumoral delivery of psh β -catenin or pshHIF1 α significantly reduced the growth of the tumor tissue compared with the delivery of control pDNA (Fig. 5A); the tumor volume was significantly suppressed by intratumoral delivery of psh β -catenin or pshHIF1 α 18 or

15 days after initiation of the therapeutic treatment, respectively. Tumor growth was suppressed in all mice treated with psh β -catenin or pshHIF1 α , and the tumor regressed markedly in two and one out of the four mice treated with psh β -catenin or pshHIF1 α , respectively, as shown in Fig. 5B–D.

4. Discussion

When B16 cells were transfected with pDNA expressing enhanced green fluorescent protein (EGFP) in vitro, a flow cytometric analysis demonstrated that about 80% of cells were EGFP positive at 24 h after transfection (unpublished data). Therefore, pDNA expressing shRNA can also be delivered to about 80% of cells in the transfection condition used, because the two plasmids are not quite different in size (3 kb for pDNA expressing shRNA and 4 kb for pDNA expressing EGFP). Transfection of psh β -catenin and pshHIF1 α was effective in suppressing corresponding target mRNA expression to about 20 or 25% of control value, respectively. Reduction in the mRNA expression of β -catenin or HIF1 α was associated with a reduced number of viable cells. There are two different mechanisms governing the reduction in the proliferation of B16 tumor cells by the suppression of β -catenin or HIF1 α expression: one is a reduced proliferation rate of B16 cells [21,22], and the other is an increased number of dead cells. To investigate whether the transfection of psh β -catenin or pshHIF1 α increases the number of dead cells, B16 cells were double-stained with annexin V conjugated with fluorescein and PI, and analyzed by flow cytometry to determine the ratio of dead cells to total cells. To analyze the growth and death rate of the transfected B16 cells, we assumed that cells proliferate and die according to first-order rate processes. The death rates of cells were calculated based on the data shown in Fig. 3D. To calculate the proliferation rates, the time course of the viable cell number after transfection was evaluated by simultaneously performing an MTT assay (data not shown). The calculated proliferation rates were 0.485 (control pDNA), 0.270 (psh β -catenin) and 0.412 (pshHIF1 α), and the death rates of the cells were 0.0286 (control pDNA), 0.0948 (psh β -catenin) and 0.0621 (pshHIF1 α). These results suggest that both the increase in cell death and the decrease in cell proliferation rate contribute to the decrease in the number of B16 cells caused by the transfection of psh β -catenin and pshHIF1 α .

We have reported that electroporation significantly (about 10-fold) increases transgene expression in tumor tissues after intratumoral injection of pDNA expressing firefly luciferase [19]. Electroporation was also effective in suppressing target gene expression after intratumoral injection of shRNA-expressing pDNA. Intratumoral injection of shRNA-expressing pDNA suppressed target gene (firefly luciferase) expression to about 30% of the control value when combined with electroporation [19], but to about 80% without electroporation (unpublished data). Therefore, the delivery efficiency of shRNA-expressing pDNA can also be significantly increased by electroporation. An intratumoral injection of psh β -catenin or pshHIF1 α followed by electroporation successfully suppressed the corresponding target gene expression to the level below

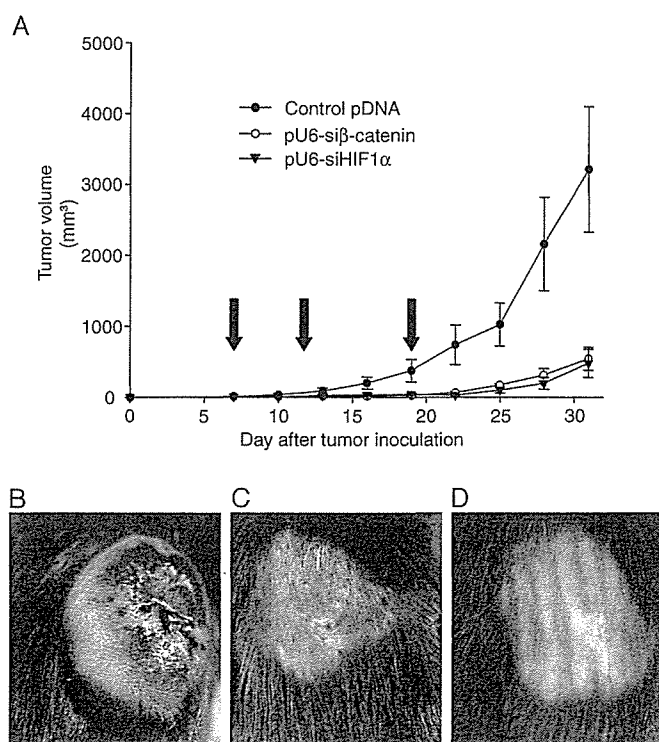


Fig. 5. Effects of intratumoral delivery of shRNA-expressing pDNAs on the growth of primary tumor tissue. (A) Mice received an intratumoral injection of 30 μ g piGENE-hU6 or shRNA-expressing pDNAs followed by electroporation. shRNA-expressing pDNAs were administered at day 7, 10 and 19 after tumor inoculation. Arrows indicate the timing of pDNA administration. The results are expressed as the mean \pm S.E.M. ($n=4$). * $P<0.05$ for Student's t -test versus control group. (B–D) Photographic image of tumor tissue of mice who received an intratumoral injection of piGENE-hU6 (B), psh β -catenin (C) or pshHIF1 α (D) at 18 days after initiation of therapeutic treatment.

30% of the control. Moreover, intratumoral delivery of psh β -catenin or pshHIF1 α also retarded *in vivo* tumor growth although the mRNA expression was not completely suppressed. Intratumoral injection of shRNA-expressing pDNAs followed by electroporation reduced target gene expression to about 30% of the control values, and the intensity of inhibitory effect was comparable with that of *in vitro* transfection, in which about 80% of cells receive plasmid DNA as mentioned above. Therefore, these results suggest that about 80% of the tumor cells receive the shRNA-expressing pDNA injected intratumorally, and that the delivery efficiency is enough to suppress tumor growth. Large tumor tissues with a diameter of over 6 mm were less sensitive to the same treatment than small ones of 2–3 mm in diameter (data not shown), suggesting the importance of the delivery efficiency of the shRNA-expressing pDNA. A combination with other therapeutic treatments, such as enhancing host immune response to tumor cells, could be an effective approach to further suppressing tumor growth.

5. Conclusion

We found that the silencing of β -catenin or HIF1 α is effective in reducing the proliferation of melanoma cells. The delivery of psh β -catenin or pshHIF1 α to intradermal tumor tissues suppressed the corresponding mRNA expression and the growth of tumor tissue. These results indicate that strategies targeting β -catenin or HIF1 α , including the use of RNAi, may be of use in the future treatment of cancer.

Acknowledgements

This work was supported in part by a Grant-in-Aid for Scientific Research from the Ministry of Education, Culture, Sports, Science and Technology, Japan and by a Health and Labor Sciences Research Grants from the Ministry of Health, Labor and Welfare of Japan.

References

- [1] P.D. Zamore, T. Tuschl, P.A. Sharp, D.P. Bartel, RNAi: double-stranded RNA directs the ATP-dependent cleavage of mRNA at 21 to 23 nucleotide intervals, *Cell* 101 (1) (2000) 25–33.
- [2] T. Tuschl, P.D. Zamore, R. Lehmann, D.P. Bartel, P.A. Sharp, Targeted mRNA degradation by double-stranded RNA *in vitro*, *Genes Dev.* 13 (24) (1999) 3191–3197.
- [3] S.M. Hammond, E. Bernstein, D. Beach, G.J. Hannon, An RNA-directed nuclease mediates post-transcriptional gene silencing in *Drosophila* cells, *Nature* 404 (6775) (2000) 293–296.
- [4] N. Kobayashi, Y. Matsui, A. Kawase, K. Hirata, M. Miyagishi, K. Taira, M. Nishikawa, Y. Takakura, Vector-based *in vivo* RNA interference: dose- and time-dependent suppression of transgene expression, *J. Pharmacol. Exp. Ther.* 308 (2) (2004) 688–693.
- [5] Y. Matsui, N. Kobayashi, M. Nishikawa, Y. Takakura, Sequence-specific suppression of *mdr1a/1b* expression in mice via RNA interference, *Pharm. Res.* 22 (12) (2005) 2091–2098.
- [6] S.M. Elbashir, J. Harborth, W. Lendeckel, A. Yalcin, K. Weber, T. Tuschl, Duplexes of 21-nucleotide RNAs mediate RNA interference in cultured mammalian cells, *Nature* 411 (6836) (2001) 494–498.
- [7] N.J. Caplen, S. Parrish, F. Imani, A. Fire, R.A. Morgan, Specific inhibition of gene expression by small double-stranded RNAs in invertebrate and vertebrate systems, *Proc. Natl. Acad. Sci. U. S. A.* 98 (17) (2001) 9742–9747 Electronic publication 2001 Jul 31.
- [8] O. Milhavet, D.S. Gary, M.P. Mattson, RNA interference in biology and medicine, *Pharmacol. Rev.* 55 (4) (2003) 629–648.
- [9] H. Gong, C.M. Liu, D.P. Liu, C.C. Liang, The role of small RNAs in human diseases: potential troublemaker and therapeutic tools, *Med. Res. Rev.* 25 (3) (2005) 361–381.
- [10] P.D. Rye, T. Stigbrand, Interfering with cancer: a brief outline of advances in RNA interference in oncology, *Tumour Biol.* 25 (5–6) (2004) 329–336.
- [11] M. Izquierdo, Short interfering RNAs as a tool for cancer gene therapy, *Cancer Gene Ther.* 12 (3) (2005) 217–227.
- [12] J.R. Bertrand, M. Pottier, A. Vekris, P. Opolon, A. Maksimenko, C. Malvy, Comparison of antisense oligonucleotides and siRNAs in cell culture and *in vivo*, *Biochem. Biophys. Res. Commun.* 296 (4) (2002) 1000–1004.
- [13] R. Kretschmer-Kazemi Far, G. Sczakiel, The activity of siRNA in mammalian cells is related to structural target accessibility: a comparison with antisense oligonucleotides, *Nucleic Acids Res.* 31 (15) (2003) 4417–4424.
- [14] A. Grunweller, E. Wyszko, B. Bieber, R. Jahnel, V.A. Erdmann, J. Kurreck, Comparison of different antisense strategies in mammalian cells using locked nucleic acids, 2'-O-methyl RNA, phosphorothioates and small interfering RNA, *Nucleic Acids Res.* 31 (12) (2003) 3185–3193.
- [15] M. Miyagishi, M. Hayashi, K. Taira, Comparison of the suppressive effects of antisense oligonucleotides and siRNAs directed against the same targets in mammalian cells, *Antisense Nucleic Acid Drug Dev.* 13 (1) (2003) 1–7.
- [16] Y. Zeng, B.R. Cullen, RNA interference in human cells is restricted to the cytoplasm, *RNA* 8 (7) (2002) 855–860.
- [17] M. Stevenson, Therapeutic potential of RNA interference, *N. Engl. J. Med.* 351 (17) (2004) 1772–1777.
- [18] L. Zender, S. Kubicka, siRNA based strategies for inhibition of apoptotic pathways *in vivo*—analytical and therapeutic implications, *Apoptosis* 9 (1) (2004) 51–54.
- [19] Y. Takahashi, M. Nishikawa, N. Kobayashi, Y. Takakura, Gene silencing in primary and metastatic tumors by small interfering RNA delivery in mice: quantitative analysis using melanoma cells expressing firefly and sea pansy luciferases, *J. Control. Release* 105 (3) (2005) 332–343.
- [20] W.J. Nelson, R. Nusse, Convergence of Wnt, beta-catenin, and cadherin pathways, *Science* 303 (5663) (2004) 1483–1487.
- [21] U.N. Verma, R.M. Surabhi, A. Schmalstieg, C. Becerra, R.B. Gaynor, Small interfering RNAs directed against beta-catenin inhibit the *in vitro* and *in vivo* growth of colon cancer cells, *Clin. Cancer Res.* 9 (4) (2003) 1291–1300.
- [22] G.L. Semenza, Targeting HIF-1 for cancer therapy, *Nat. Rev., Cancer* 3 (10) (2003) 721–732.
- [23] X. Sun, J.R. Kanwar, E. Leung, K. Lehnert, D. Wang, G.W. Krissansen, Gene transfer of antisense hypoxia inducible factor-1 alpha enhances the therapeutic efficacy of cancer immunotherapy, *Gene Ther.* 8 (8) (2001) 638–645.
- [24] L. Li, X. Lin, M. Staver, A. Shoemaker, D. Semizarov, S.W. Fesik, Y. Shen, Evaluating hypoxia-inducible factor-1alpha as a cancer therapeutic target via inducible RNA interference *in vivo*, *Cancer Res.* 65 (16) (2005) 7249–7258.
- [25] R. Supino, MTT assays, *Methods Mol. Biol.* 43 (1995) 137–149.

Enhanced antigen-specific antibody production following polyplex-based DNA vaccination via the intradermal route in mice

Atsushi Kawase, Keiko Isaji, Ayumi Yamaoka, Naoki Kobayashi,
Makiya Nishikawa, Yoshinobu Takakura*

*Department of Biopharmaceutics and Drug Metabolism, Graduate School of Pharmaceutical Sciences,
Kyoto University, Sakyo-ku, Kyoto 606-8501, Japan*

Received 16 June 2005; received in revised form 24 April 2006; accepted 25 April 2006
Available online 5 May 2006

Abstract

DNA vaccination is an attractive approach with various advantages over conventional vaccination. The present study was undertaken to examine whether polyplex-based DNA vaccination could be used to modulate immune responses by plasmid DNA (pDNA). Methylated bovine serum albumin (mBSA) was used as a model of a cationic macromolecular carrier of pDNA encoding ovalbumin (OVA) and the effects of polyplex formation of pDNA with mBSA on the antigen-specific immune responses were examined. Anti-OVA IgG antibody production was significantly increased following intradermal immunization with the polyplex compared with naked pDNA, although the induction of cytotoxic T lymphocyte activity was lowered by polyplex formation. We also demonstrated that the disposition and gene expression of pDNA following intradermal injection could be manipulated by polyplex formation. Intriguingly, we also found that the migration of dendritic cells to the injected site could be induced by polyplex formation probably due to a high level of tumor necrosis factor α production from the keratinocytes treated with mBSA/pDNA complexes. Thus, the present study has demonstrated that the immune responses could be biased towards a Th2-type response by polyplex-based DNA vaccination through manipulation of not only pDNA disposition but also dendritic cell migration.

© 2006 Elsevier Ltd. All rights reserved.

Keywords: DNA vaccine; Polyplex; Dendritic cell

1. Introduction

DNA vaccination is the approach that can induce both humoral and cellular immune responses against various diseases by injection of plasmid DNA (pDNA) encoding antigen [1,2]. These responses include protective neutralizing antibodies and antigen-specific cytotoxic T lymphocytes (CTL). Professional antigen presenting cells, such as dendritic cells (DC), most likely play a key role in initiating primary immune responses after DNA vaccination [3,4]. The induction of antigen-specific immune responses occurs through the presentation of appropriate peptides in the context of major histocompatibility polyplex (MHC) molecules on DC. In general,

DC appear to play at least three distinct roles in genetic immunization: (1) MHC class II-restricted presentation of antigens that are secreted by the neighboring, transfected somatic cells; (2) MHC class I-restricted, “cross-presentation” of antigens that are released by the transfected somatic cells; and (3) direct presentation of antigens that are produced endogenously in the transfected DC themselves. We hypothesized that antigen-specific immune responses depending on these processes could be modulated by manipulation of the profiles of local disposition of pDNA and subsequent protein expression following immunization by polyplexation with cationic macromolecules.

In this study, we investigated the effect of polyplex formation on the antigen-specific immune responses induced by DNA vaccination to test this hypothesis. We prepared a pDNA/cationic polymer polyplex, i.e., polyplex, using

* Corresponding author. Tel.: +81 75 753 4615; fax: +81 75 753 4614.
E-mail address: takakura@pharm.kyoto-u.ac.jp (Y. Takakura).

pDNA encoding ovalbumin (OVA) expressing plasmid [5] and methylated bovine serum albumin (mBSA), which has been shown to act as an adjuvant [6,7].

We performed the immunization via the intradermal route because skin contains numerous, readily accessible cutaneous DC [epidermal Langerhans cell (LC) and dermal DC] and the keratinocytes (KC) which account for 90–95% of the cells in the epidermis are known to produce proinflammatory cytokines, such as interleukin (IL)-1, tumor necrosis factor α (TNF- α) and granulocyte-macrophage colony stimulating factor (GM-CSF) in response to allergens, infection, or injury [8]. These cytokines can promote DC and LC maturation, and are taken up from the blood and migrate to regional lymph nodes where antigenic peptides presented to naïve T cell and primary T cell responses are triggered [9,10].

The present study suggests that the anti-OVA IgG antibody response, the Th2-type response, is enhanced by polyplex formation. We have also shown that polyplex formation significantly affects the local disposition and subsequent transgene expression of pDNA following intradermal injection. Intriguingly, we have also found that polyplex administration induces DC accumulation in the injection site. It was found that the disposition of pDNA and DC in treated skins could be modified by polyplex formation. Thus, the present study demonstrates that the immune responses can be modulated by polyplex-based DNA vaccination through manipulation of not only pDNA disposition but also dendritic cell migration.

2. Materials and methods

2.1. Mice

Five- to six-week old female ddY or C57BL/6 (immunization experiment) mice were purchased from Japan SLC Co. (Shizuoka, Japan) and maintained under conventional housing conditions. Mice were anesthetized by inhalation of ether and euthanized by cervical dislocation.

2.2. Plasmid DNA

In the immune response experiments, we used pDNA encoding ovalbumin (OVA), pOVA, as a model antigen-expressing pDNA. pOVA was a kind gift from Dr. Shoshana Levy (Department of Medicine/Oncology, Stanford University Medical Center, Stanford USA). In the gene expression experiments, we used pLuc containing the firefly luciferase gene under the control of the CMV promoter. The pDNA was constructed by subcloning the *HindIII/XbaI* firefly luciferase cDNA fragment from pGL3-control vector into the polylinker of the pcDNA3 vector. In the confocal microscopic study, we used pGeneGripTM (Rhodamine/GFP) (Gene Therapy Systems, San Diego, CA, USA) to observe co-localization of pDNA and transgene expression.

The pDNA amplified in the *DH5 α* strain of *Escherichia coli* was extracted and purified using a QIAGEN EndofreeTM

Plasmid Giga Kit (QIAGEN GmbH, Hilden, Germany). The purity was checked by 1% agarose gel electrophoresis followed by ethidium bromide staining. The pDNA concentration was measured by UV absorption at 260 nm. To minimize activation by contaminated lipopolysaccharide (LPS) for in vitro experiments (Fig. 10), DNA samples were purified extensively with Triton X-114 (Nacalai Tesque, Kyoto, Japan), a non-ionic detergent [11,12]. DNA samples were purified by extraction with phenol:chloroform:isoamyl alcohol (25:24:1) and ethanol precipitation. DNA (10 mg) was diluted with 20 mL pyrogen-free water, and then 200 μ L Triton X-114 was added followed by mixing. The solution was placed on ice for 15 min and incubated for 15 min at 55 °C. Subsequently, the solution was centrifuged for 20 min at 25 °C, 600 \times g. The upper phase was transferred to a new tube, 200 μ L Triton X-114 was added, and the previous steps were repeated three or more times. The activity of LPS was measured by limulus amoebocyte lysate (LAL) assay using the Limulus F Single Test kit (Wako, Tokyo, Japan). After Triton X-114 extraction, the endotoxin levels of DNA samples could no longer be determined by LAL assay; i.e., 1 μ g/mL DNA contained less than 0.001 EU/mL. Without extraction of endotoxin by Triton X-114, 100 μ g/mL naked pDNA, which contains 1–5 EU/mL endotoxin, could release 521 \pm 73 pg/mL TNF- α over 24 h.

2.3. Preparation of mBSA/pDNA complexses

mBSA was synthesized from BSA (96–99%, standard grade) (Sigma, St. Louis, MO, USA) according to an earlier report [13]. Briefly, BSA was mixed with absolute methyl alcohol under acidic conditions (hydrochloric acid). In this process, the carboxyl group of the acidic amino acids in BSA was esterified and BSA was converted to a cationic macromolecule; the yield from this reaction was virtually 100%. mBSA/pDNA complexses were prepared by adding various amounts of mBSA to pDNA to give different charge ratios (+/–). The final concentration of pDNA was adjusted to 0.1 μ g/ μ L in 5% dextrose.

2.4. Immunization

Female C57BL/6 mice were injected intradermally in the dorsal region with 20, 40 (Fig. 2) or 100 μ g (Figs. 2 and 4) pOVA or pOVA polyplexed with mBSA at biweekly intervals or only a single application was given. Control animals received 100 μ g OVA protein (Sigma, St. Louis, MO, USA) emulsified in complete Freund's adjuvant (CFA) [14] (ICN Biomedicals Inc. Aurora, OH, USA) intraperitoneally.

2.5. Determination of total IgG and IgG1 or IgG2a subclass of anti-OVA antibodies titers by enzyme-linked immunosorbent assay

Serum samples were collected from the tail vein of mice to determine anti-OVA IgG, IgG1 and IgG2a antibodies titers.

The levels of antibodies were measured by enzyme linked immunosorbent assay (ELISA). OVA (1 mg/mL) in carbonate/bicarbonate buffer (0.1 M, pH 9.6) was distributed to each well of 96-well flat-bottom polystyrene plates (100 μ L/well). Following overnight incubation at 4 °C, wells were blocked with 5% BSA-containing Tween-20 phosphate buffered saline (T-PBS) [0.5% (w/w) Tween-20 (ICN Biomedicals Inc. Aurora, OH, USA) in PBS] for 30 min at 37 °C. After the wells were washed three times with T-PBS, serially diluted 100 μ L serum samples were added to the wells. After 2 h incubation at 37 °C, the wells were washed five times with T-PBS and 100 μ L anti-IgG, IgG1 or IgG2a-HRP conjugate (Sigma, St. Louis, MO, USA), diluted 2000:1 with 5% BSA-containing T-PBS, was added to each well. After a 2 h incubation, each well was washed with T-PBS and then 200 μ L freshly prepared *o*-phenylenediamine dihydrochloride (Wako, Tokyo, Japan) solution in phosphate-citrate buffer (0.05 M, pH 5.0) was added to each well. After a 30 min incubation, 50 μ L 10% H₂SO₄ was added and then the absorbance was measured at 490 nm. Serum total IgG, IgG1 and IgG2a titers were estimated by the dilution ratio at which an absorbance value of 0.1 was obtained.

2.6. CTL assay

In the CTL assay, we used EL4 and E.G7 (EL4 expressing OVA) as target cells. EL4 cells were cultured in Dulbecco's modified Eagle medium (Nissui Pharmaceutical, Tokyo, Japan) supplemented with 10% heat-inactivated fetal bovine serum (FBS) (Thermo Trace, Melbourne, Australia), 2 mM L-glutamine and antibiotics. E.G7 cells were cultured in RPMI 1640 medium supplemented with 10% heat-inactivated FBS, 50 μ M 2-mercaptoethanol (2-ME) (Sigma, St. Louis, MO, USA), 2 mM L-glutamine, glucose, sodium pyruvate, HEPES (Nacalai Tesque, Kyoto, Japan) and G418. Immunization was performed three times at biweekly intervals. One week after the last immunization, spleen cells were isolated from the immunized mice and restimulated *in vitro* for 5 days with mitomycin C-treated E.G7. Target cells were labeled with ⁵¹Cr by incubating with Na₂⁵¹CrO₄ (Daiichi Radioisotope Labs, Tokyo, Japan) in culture medium for 45 min at 37 °C. After washing, 2 \times 10⁴ of the ⁵¹Cr-labeled target cells and serially diluted spleen cells were coincubated in 200 μ L culture medium for 4 h at 37 °C. Spontaneous release of ⁵¹Cr without effector cells and maximal release in the presence of 1% NP40 were also evaluated. Cells were centrifuged (1500 rpm) for 5 min, and 100 μ L of each supernatant was collected for radioactivity measurements. The cytolytic activity of CTL was calculated as [15]:

% killing

$$= 100 \times \frac{(\text{observed release} - \text{spontaneous release})}{(\text{maximal release} - \text{spontaneous release})}$$

2.7. Determination of cytokine production from spleen cells and proliferation of antigen-specific T cells

At 4 weeks after the final immunization, spleen cells isolated from immunized mice were cocultured with OVA protein in RPMI 1640 medium supplemented with 10% heat-inactivated fetal FBS, 10 mM HEPES, 1 mM sodium pyruvate, 0.1 mM non-essential amino acids, 2 mM L-glutamine and 50 mM 2-ME at 37 °C for 3 days. The levels of cytokines (IL-12, IL-10 and IL-4) released into the culture medium were measured by a suitable ELISA kit (ANALYZA mouse IL-12, IL-10 and IL-4, genzyme TECHNE, Minneapolis, MN, USA). The proliferation of antigen-specific T cells was determined by Alamar Blue assay (Alamar BioSciences, Sacramento, CA, USA), based on the bioreduction of a fluorogenic substrate.

2.8. *In vivo* reporter gene assay after intradermal administration

A 1.5 cm \times 1.5 cm area of skin was removed from each mouse at 1 or 3 days after intradermal administration of naked pLuc or mBSA/pLuc polyplexes. Tissues were homogenized with lysis buffer [0.1 M Tris (Wako, Tokyo, Japan), 0.05% Triton X-100 (Nacalai Tesque, Kyoto, Japan), 2 mM EDTA (Wako, Tokyo, Japan), pH 7.8], and subjected to three cycles of freezing (−190 °C) and thawing (37 °C). The homogenates were centrifuged at 14,000 \times g for 8 min at 4 °C. Ten μ L supernatant was mixed with 100 μ L luciferase assay buffer (Picagene, Toyo Ink, Tokyo, Japan) and the chemiluminescence produced was measured in a luminometer (Lumat LB 9507, EG & G Berthold, Bad Wildbad, Germany).

2.9. Confocal microscopic studies of localization of pDNA and expressed proteins

Mice (female ddY) were injected with 20 μ g pGeneGripTM (Rhodamine/GFP) intradermally. We could observe the disposition of both pDNA and expressed protein because this pDNA is rhodamine-labeled pDNA encoding GFP. At 1 or 24 h after injection, mice were euthanized and their skins were excised. Cryosections, 10 μ m thick, were prepared using a cryostat (Jung Frigocut 3000E, Leica Microsystems AG, Wetzlar, Germany) and fixed in 10% neutral formalin. The sections were examined by confocal microscopy (MRC-1024, BioRad, Hercules, CA, USA).

2.10. Flow cytometric analysis of the presence of CD11c⁺ cells in skin

In this experiment, 20 μ g pOVA or pOVA polyplexed with mBSA (8:1) was injected into the skin. After 6 h, the skin was excised and treated with 1% trypsin (Invitrogen Corp., Carlsbad, CA USA) for 1 h at 37 °C. Following removal of the epidermis from the dermis, it was treated in 0.025%

DNase I (Sigma, St. Louis, MO, USA) for 20 min. The cells of the treated epidermis were extruded using a sterilization stick and washed three times in RPMI 1640. After the supernatant was removed, the obtained KC were resuspended in 150 μ L PBS containing 0.5% BSA per 10^8 total cells. The cell suspension was mixed with 50 μ L (2 μ g) fluorescein isothiocyanate (FITC)-conjugated anti-mouse CD11c antibody (BD Biosciences, USA) and incubated for 15 min at 4 °C. After adding 10 mL PBS, the supernatant was removed and the cells were resuspended in 500 μ L PBS. Flow cytometric analysis to detect the presence of CD11c⁺ cells in the skin was performed using a FACSCalibur cytometer (Becton Dickinson, San Jose, CA, USA) and cellquest software (Becton Dickinson, San Jose, CA, USA). We confirmed that there was a significant difference between the histograms of pOVA and that of mBSA/pOVA (8:1) by CellQuest software (Becton Dickinson).

2.11. Accumulation of CD11c⁺ cells in treated skins of immunized mice

Injections of 20 μ g of pOVA or pOVA polyplexed with mBSA (8:1) were made into the skin and, after 6 h, the skin cells were isolated. We used murine bone marrow-derived dendritic cells (BMDC) after differentiation of cells isolated from murine bone marrow. After the bone marrow was flushed out from the bones of the murine hind legs, the cells were cultured in RPMI 1640 medium supplemented with 10% FBS and 1000 U/mL rGM-CSF. After 4 to 5 days incubation at 37 °C in 5% CO₂–95% air, cells were collected and centrifuged at 200 \times g for 10 min. After the supernatant was removed, the cells were resuspended in 400 μ L of PBS containing 0.5% BSA per 10^8 total cells. The cell suspension was mixed with 100 μ L mouse CD11c MicroBeads (Miltenyi Biotec, Germany) and incubated for 15 min at 4 °C. CD11c is one of the differentiation antigens of DC. Cells were washed, centrifuged at 200 \times g for 10 min, and resuspended in 500 μ L PBS containing 0.5% BSA. Then, magnetic separation with magnetic cell sorting (MACS) (autoMACS, Miltenyi Biotec, Germany) was carried out to isolate DC, by selecting CD11c-positive (+) cells from all the cultured cells. We confirmed that the recovery efficacy of the CD11c⁺ cells was not variable between preparations by preliminary experiments.

2.12. Determination of TNF- α release from cultured KC

KC isolated as described in the flow cytometric analysis were cultured with Keratinocyte-SFM (Invitrogen Corp., Carlsbad, CA USA) in 24-well plates. After washing three times with 0.5 mL Keratinocyte-SFM, 1.5 μ g pOVA or pOVA polyplexed with mBSA (8:1) was transfected. After 18 h incubation, the supernatant was collected and the concentration of TNF- α was analyzed by ELISA (ANALYZA mouse TNF- α , genzyme TECHNE, Minneapolis, MN, USA).

2.13. Statistics

Significant differences between mean values of the levels of gene expression were estimated using the Student's paired *t*-test after ANOVA.

3. Results

3.1. Determination of total IgG and IgG1 or IgG2a subclass of anti-OVA antibodies titers

We investigated the effects of polyplex formation on the types of immune responses induced by DNA vaccination. Antigen-specific immune responses induced following DNA vaccination include CTL induction and antibody production. To examine whether the antigen-specific antibody production was affected by polyplex formation, we measured the

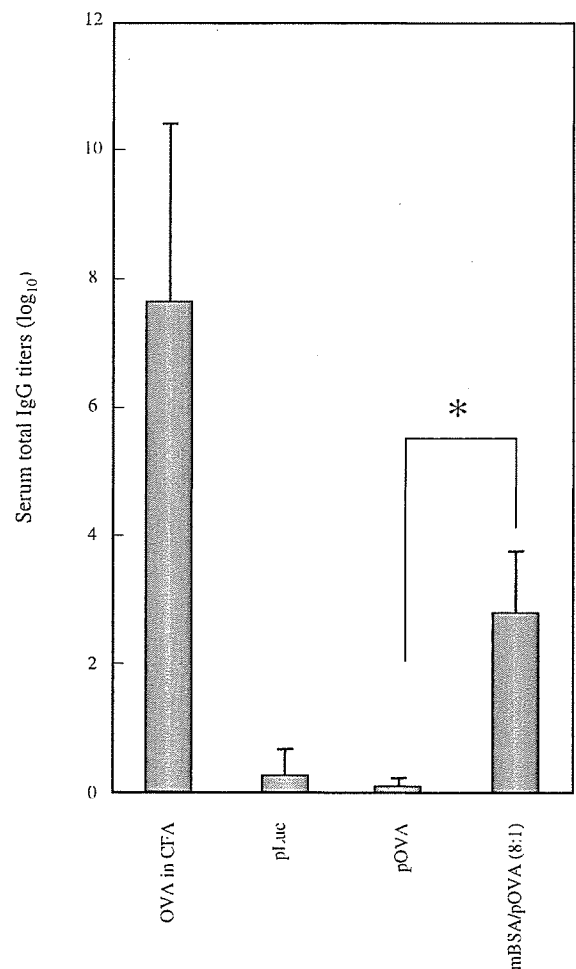


Fig. 1. Production of total anti-OVA IgG antibody at 6 weeks after single immunization of pOVA or mBSA/pOVA polyplexes (8:1) via the intradermal route. The serum samples from immunized mice were collected and the antibody titers were measured by ELISA. The results are expressed as mean \pm S.D. of four mice. *Indicates a significant difference between the values of pOVA and mBSA/pOVA (8:1) ($p < 0.01$).

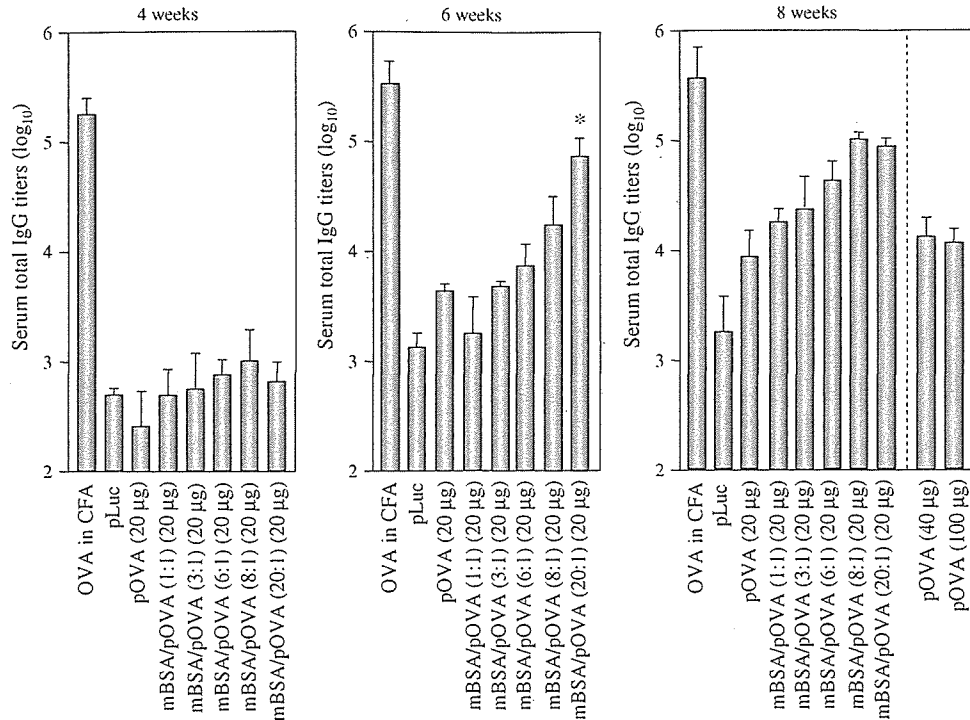


Fig. 2. Production of total anti-OVA IgG antibody after biweekly immunization of pOVA or mBSA/pOVA polyplexes via the intradermal route. The serum samples from immunized mice were collected and the antibody titers were measured by ELISA. The results are expressed as mean \pm S.D. of four mice. *Indicates a significant difference between the values of pOVA and mBSA/pOVA (20:1) ($p < 0.01$).

amount of anti-OVA IgG antibodies in immunized mice. Fig. 1 shows the total anti-OVA IgG antibody level after a single immunization. A significantly increased level of total anti-OVA IgG antibody was obtained in mice immunized with mBSA/pOVA polyplexes (8:1), whereas little antibody response was detected in mice immunized with naked pOVA. We also examined the total IgG level following biweekly immunization with polyplexes with different charge ratios (Fig. 2). A marked increase in IgG titers was obtained by biweekly intradermal administration of mBSA/pOVA polyplexes, particularly at the higher charge ratios. In the mBSA/pOVA polyplexes (8:1) or (20:1), the levels of antibody were increased up to 4.0 or 15.7 times at 6 weeks and up to 11.5 or 11.0 times at 8 weeks, respectively, compared with that of naked pOVA. It was also found that the levels of IgG antibody production in mice treated with mBSA/pOVA polyplexes were higher than those in mice treated with higher doses (40 or 100 µg) of naked pOVA. These results show that the required dose of pDNA and the required number of immunizations to induce an antibody response can be reduced by polyplex formation. Further, we examined the subclass of anti-OVA IgG antibody to determine the type of promoted immune responses (Fig. 3). The levels of anti-OVA IgG2a antibody production were similar in mice treated with polyplexes and naked pDNA. On the other hand, a significant production of anti-OVA IgG1 antibody was detected in mice treated with mBSA/pOVA polyplexes but not in mice treated with naked pOVA at the same dose, indicating

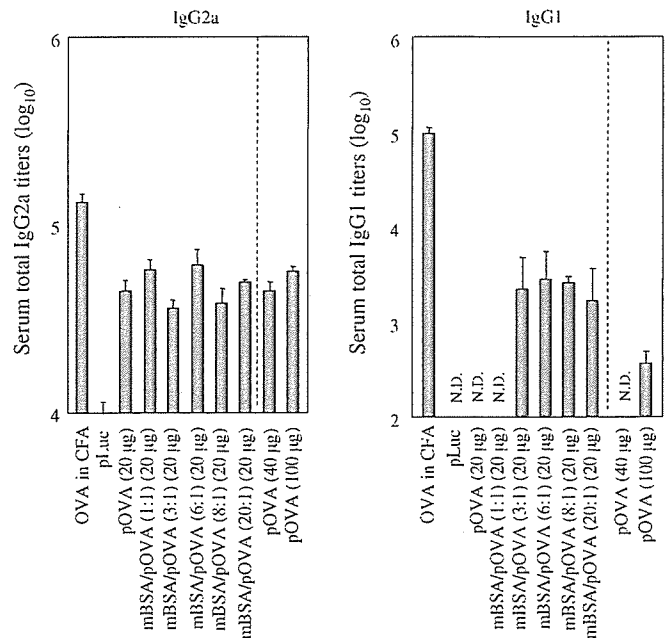


Fig. 3. Production of IgG1 or IgG2a subclasses of anti-OVA antibody at 8 weeks after biweekly immunization of pOVA or mBSA/pOVA polyplexes via the intradermal route. The serum samples from immunized mice were collected and the antibody titers were measured by ELISA. The results are expressed as mean \pm S.D. of four mice.

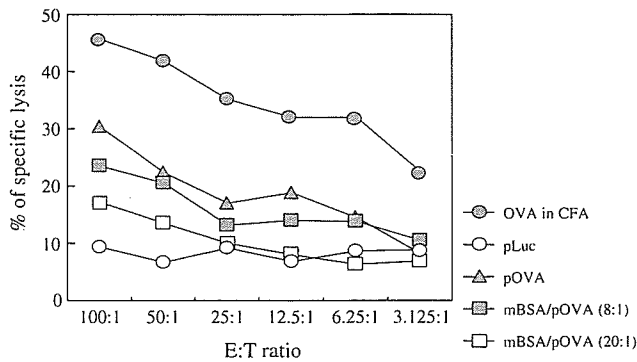


Fig. 4. Generation of OVA-specific CTL by immunization with pOVA or mBSA/pOVA polyplexes via the intradermal route. Mice were immunized four times with 100 μ g pOVA or pOVA polyplexed with mBSA. Seven days after the last immunization, spleen cells were isolated and a standard 51 Cr-release assay was performed using the spleen cells cultured for 5 days.

that Th2-type immune responses are promoted by polyplex formation.

3.2. CTL assay

As the effect of polyplex-based DNA vaccination on antibody responses was demonstrated, we next examined whether this approach could affect the CTL response. In the experiment involving the CTL assay, we used mBSA/pOVA polyplexes (8:1) and (20:1) which showed an enhanced antibody response (Fig. 2). The activities of antigen-specific CTL response against E.G7 obtained by these polyplexes were slightly reduced compared with that obtained by naked pOVA

(Fig. 4). We confirmed the antigen specificity by the minor degree of cell killing detected in EL4 (data not shown). The cpm values of spontaneous release and maximal release were 540.4 and 6568, respectively.

3.3. Determination of cytokine production from spleen cells and proliferation of antigen-specific T cells

To clarify the effect of polyplex-based DNA vaccination on immune responses, we investigated the responsiveness of spleen cells from immunized mice against OVA protein, although the analysis of sentinel lymph node also may provide additional information. We determined the levels of cytokine production from the spleen cells pulsed with OVA protein in Fig. 5A. The levels of IL-10 and IL-4 (Th2-type cytokines) released from spleen cells were increased by polyplex formation although the levels of IL-12 (Th1-type cytokine) scarcely changed. Fig. 5B shows that the proliferation of antigen-specific T cells was also promoted by polyplex formation, suggesting that the immune system was activated following polyplex-based DNA vaccination.

3.4. Reporter gene assay after intradermal administration

We demonstrated that the immune responses induced by DNA vaccination could be modulated by polyplex formation. We assumed that the gene expression and the disposition of pDNA following local injection were significantly altered by polyplex formation and these alterations would affect the immune responses. To examine whether the levels of trans-

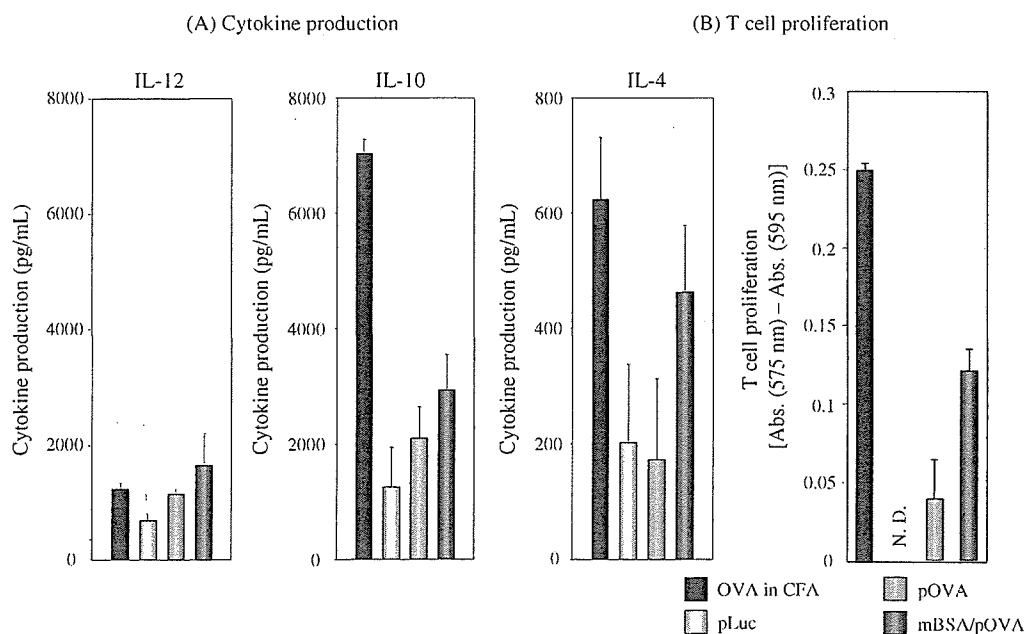


Fig. 5. (A) production of cytokines from spleen cells and (B) proliferation of antigen-specific T cells after immunization of pOVA or mBSA/pOVA polyplexes (A; 20:1, B; 6:1). (A) At 4 weeks after the final immunization, spleen cells isolated from immunized mice were co-cultured with OVA protein at 37 °C for 3 days. The levels of cytokines release into the culture medium were measured by ELISA. The results are expressed as mean \pm S.E.M. of three wells. (B) The proliferation of antigen-specific T cells was determined by Alamar Blue assay. The results are expressed as mean \pm S.D. of three wells.

gene expression were affected by polyplex formation, we carried out *in vivo* quantitative gene expression experiments using pDNA encoding luciferase (pLuc). We measured the levels of gene expression in the skin at 1 or 3 days after administration (Fig. 6). Intradermal administration of naked pLuc resulted in a relatively high level of gene expression. A similar level of gene expression was obtained by intradermal administration of mBSA/pLuc polyplexes (1:1). On the other hand, the levels of gene expression were dramatically reduced in mBSA/pLuc polyplexes (3:1), (6:1), (8:1) and (20:1) depending on the mixing ratio, indicating that polyplex formation significantly reduced transgene expression at the injection site (Fig. 6).

3.5. Confocal microscopic studies of localization of pDNA and expressed protein

The disposition of pDNA and expressed proteins is important for the induction of immune responses. To investigate whether the localization of pDNA and expressed protein was affected by polyplex formation, we examined the tissue sections by confocal microscopy at 1 and 24 h following intradermal administration of pGeneGrip™ (Rhodamine/GFP) or mBSA/pGeneGrip™ polyplexes (8:1) which showed a high antibody response (Figs. 1 and 2) and a very low level of gene expression (Fig. 6). Red signals derived from naked rhodamine-labeled pDNA were observed in the dermis at 1 h (Fig. 7A and B). In the case of the mBSA/pGeneGrip™ polyplexes (8:1), we observed that a greater number of red signals remained in the vicinity of the injection site (Fig. 7B). This

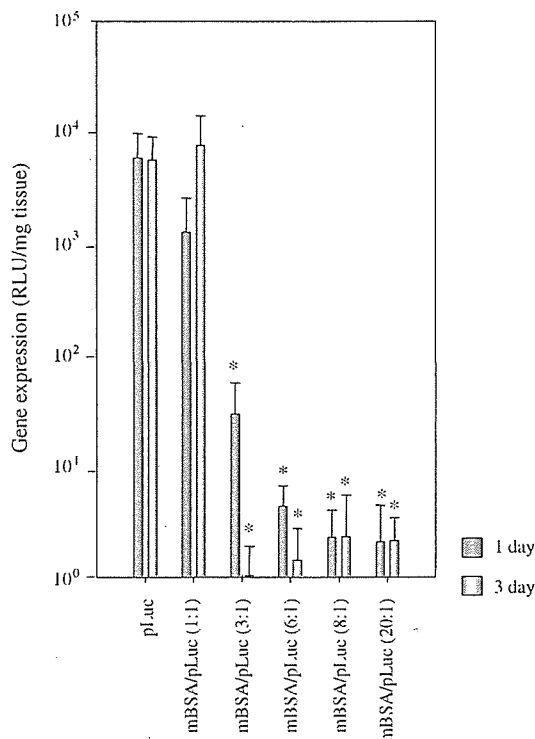


Fig. 6. Gene expression at 1 or 3 days after intradermal administration of pLuc or mBSA/pLuc at various charge ratios. The luciferase assay was performed on a 1.5 cm × 1.5 cm area of skin removed from each mouse. Four mice were used per group and the results are expressed as the mean ± S.D. *Indicates a significant difference (*p* < 0.01).

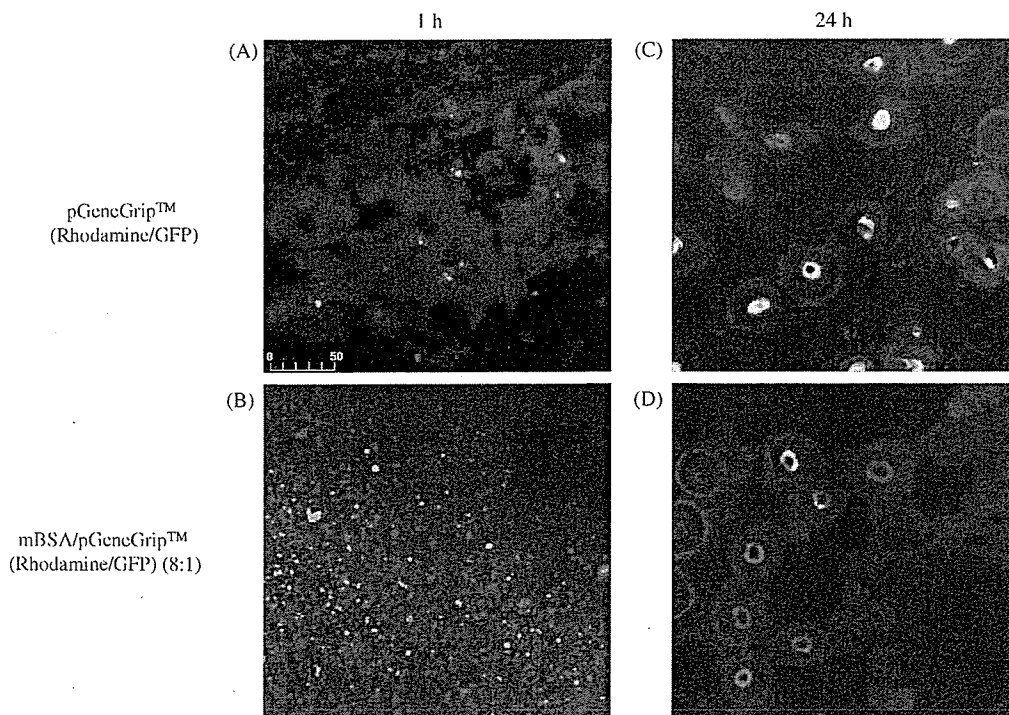


Fig. 7. Confocal microscopic images of a tissue section of mouse dorsal skin 1 or 24 h after intradermal administration of 20 μg pGeneGrip™ (rhodamine/GFP) (A) (×400) or pGeneGrip™ polyplexed with mBSA (3:1) (B) (×400).

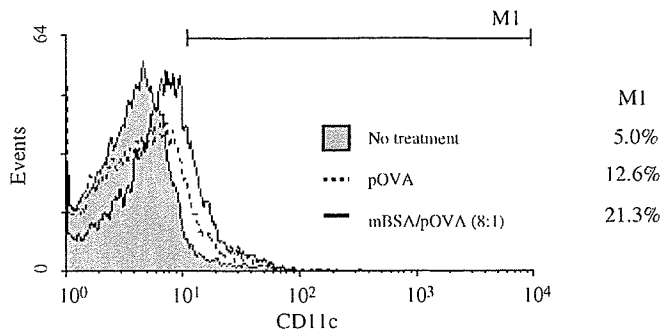


Fig. 8. Flow cytometric analysis of the presence of CD11c⁺ cells in skin. Mice were given injections of 20 µg of pOVA or mBSA/pOVA polyplexes (8:1) into the skin. After 6 h, the isolated epidermis cells were treated with FITC-conjugated anti-mouse CD11c antibody and subjected flow cytometric analysis.

result suggests that the elimination of pDNA from the treated site was retarded by polyplex formation probably due to the electrostatic interaction with the tissue and the prevention of pDNA degradation there. At 24 h, green signals derived from GFP were observed in both images (Fig. 7C and D). A higher amount of GFP protein was observed in naked pGeneGripTM (Fig. 7C). This result shows that the level of gene expression at the injection skin was reduced by polyplex formation and this agrees with the results shown in Fig. 6.

3.6. Accumulation of CD11c⁺ cells in treated skins of immunized mice

DC migration is one of the key events in the induction of immune responses. We speculated that polyplex formation might affect not only pDNA disposition/gene expression but also DC migration to the treated skin, which may be another factor modulating the immune responses. We investigated the effect of polyplex formation on the accumulation in the treated skin of endogenous DC after intradermal administration. Fig. 8 shows the results of the flow cytometric analysis. The ratio of CD11c⁺ cells per 10,000 cells in the skin treated with mBSA/pOVA (8:1) was higher than that of the control or naked pOVA. We also measured the number of CD11c⁺ cells in the treated skins using the MACS procedure (Fig. 9).

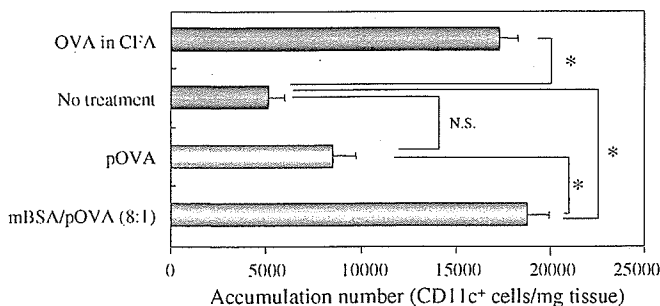


Fig. 9. Accumulation of CD11c⁺ cells in the treated skin of immunized mice at 6 h after intradermal administration of pOVA or mBSA/pOVA polyplexes. *Indicates a significant difference ($p < 0.01$). N.S.; not significant.

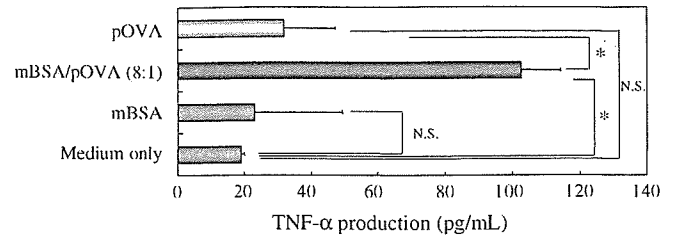


Fig. 10. Production of TNF-α from KC at 12 h after transfection of 5.0 µg pOVA, mBSA/pOVA polyplexes (8:1). The results are expressed as mean ± S.D. of six wells. *Indicates a significant difference ($p < 0.01$). N.S.; not significant.

In the case of naked pOVA, the number of CD11c⁺ cells was not significantly increased compared with no treatment. The number of accumulated CD11c⁺ cells was confirmed to increase significantly following injection of the polyplex. These results indicate that the number of DC in the treated skin was increased by polyplex formation, suggesting that mBSA/pDNA complexes are efficiently taken up by these migrating DC.

3.7. Determination of TNF-α release from cultured KC

It is known that various cytokines, including TNF-α and IL-1β, are involved in DC migration. In particular, TNF-α mainly acts by producing accumulation of DC in the skin. We carried out an *in vitro* experiment using keratinocytes (KC) in primary culture to examine whether TNF-α release occurs from KC in Fig. 10. pOVA or mBSA alone did not induce any significant level of TNF-α from the cultured KC. In contrast, mBSA/pOVA polyplexes (8:1) stimulated the KC to produce a significant amount of TNF-α. It is likely that this TNF-α production from KC is one of the important factors governing the induced accumulation of DC in treated skins *in vivo*.

4. Discussion

DNA vaccines produce both CTL induction and antibody production against encoded antigens. Each response also exerts a mutual action to control the balance of the immune responses [16,17]. To optimize immunotherapy, it is important to adjust the appropriate immune responses for various diseases. In this study, we investigated the effect of polyplex-based DNA vaccination on immune responses based on the consideration that the disposition and subsequent gene expression after local administration of pDNA are important factors determining the immune responses. Little information is available on polyplex-based DNA vaccination [18,19]. We used mBSA as a model cationic macromolecule and prepared the corresponding polyplex.

The present study has demonstrated that the anti-OVA IgG antibody responses are significantly increased in mice

immunized with the polyplex (Figs. 1 and 2), indicating that mBSA is a useful carrier for production of antibody. On the other hand, CTL activity induced by the polyplex is reduced (Fig. 4). It has been also shown that productions of IgG1 subclass of anti-OVA antibody (Fig. 3) and IL-10 and IL-4 from the spleen cells (Fig. 5) are increased. Our results suggest that the antigen-specific antibody production by polyplex immunization was increased under Th2 cytokine environment. Recent report has also demonstrated that CD8⁺ and CD8⁻ DC subsets could induce CTL response with higher Th2 cytokines [20].

The present study also demonstrated that the levels of gene expression in the injection site were dramatically reduced compared with naked pDNA (Figs. 6 and 7). This observation was somewhat unexpected because antibody production was increased. We previously reported the effects of complex formation on the disposition and gene expression after intramuscular injection [21]. Similar effects would be expected in the case of intradermal injection. We consider that the increased antibody production would be ascribed to (1) improvement of retention of pDNA in the treated skins and disposition of pDNA in the regional lymph nodes, (2) elevation of the accumulation of DC to the treated skins, (3) prevention of pDNA from degradation.

Our previous *in vitro* study demonstrated that pDNA complexed with mBSA enhanced transfection efficiency in DC2.4 cells, murine DC cell line [21]. However, *in vivo* pDNA delivery by cationic complex would lead to restricted distribution of pDNA in the skin compared with naked pDNA that could widely distribute throughout the skin and show a higher gene expression in keratinocytes, but not in DC. We speculated that the levels of gene expression in DC were increased by complex formation in not only *in vitro* but also *in vivo* condition. However, the levels of gene expression of DC in the skin did not contribute to the overall level of gene expression in the entire skin because the number of DC in skin is very low. Therefore, overall gene expression in the injection site *in vivo* was significantly decreased compared with naked pDNA (Figs. 6 and 7).

Increased antibody production might be explained, at least in part, by the interesting phenomenon that significant accumulation of DC in the treated skin occurred following polyplex injection (Figs. 8 and 9). *In vitro* experiments using cultured KC suggest that TNF- α production from KC upon stimulation with the polyplex is one of the important factors governing the induction of DC accumulation. In addition to the prolonged retention of the polyplex at the injection site (Fig. 7), this DC accumulation would be advantageous for direct interaction of pDNA with DC. We speculated that the efficiency of pDNA uptake by DC was improved at the injection site treated with mBSA/pDNA complexes. In our previous study, we showed that the levels of *in vitro* gene expression and cytokine induction in DC2.4 cells were increased by polyplex formation [21]. Although attention has to be paid to the interpretation of the data obtained under *in vivo* and *in vitro* conditions, it is possible that pDNA would

be efficiently delivered to DC *in vivo* by polyplex formation and the efficiency of direct priming in the induction of immune responses might be improved. Our previous study also demonstrated prolonged retention of pDNA in the treated skins and enhanced accumulation of pDNA in the regional lymph nodes, which might be involved in increased direct interaction of pDNA with DC.

Another possible factor for improved antibody production may be induction of substance P in the treated skins. It is reported that cationic peptide/molecules stimulate sensory nerves in dermis, resulted in releasing substance P and stimulating mast cells [22–24]. Therefore, mBSA, cationic macromolecule used in this study, might have similar biological functions. Substance P can stimulate keratinocytes and activation of mast cells also may affect induction of immune responses. Even if this was the case, the level of Substance P or mast cell activation was not so high because we observed little edema or damage in the treated skins under the microscope.

The detailed mechanism for the accumulation of DC and LC induced by polyplex injection is unknown. KC participates in cutaneous immune responses by producing various cytokines. Topical exposure of mice to contact allergens and skin irritants is known to stimulate the upregulated expression of various epidermal cytokines, including IL-1 β , IL-6, TNF- α , GM-CSF and macrophage inflammatory protein 2 (MIP-2). Among them, IL-1 β , TNF- α and IL-6 are known to provide mandatory signals for the mobilization of DC and LC. In the epidermis, KC is the main source of TNF- α , although other cell types may also produce a small amount of this cytokine. Immature DC express CC chemokine receptor 6 (CCR6). The ligands for CCR6, MIP-3 α and defensins- β , are expressed in KC and migration of DC occurs depending on the ligand-receptor interaction. It has been reported that the expression of MIP-3 α and defensins- β are enhanced by TNF- α from KC [25,26]. TNF- α also stimulates vascular endothelial cells in inflammatory sites and increases the expression of vascular cell adhesion molecule-1 (VCAM-1), which can facilitate DC accumulation in local tissue from the blood circulation. These processes would be involved in the DC accumulation observed in the present study.

A number of mechanisms of TNF- α production from KC have been reported [27–29]. KC constitutively express various members of the toll-like receptor (TLR) family, such as TLR1, TLR2, TLR3, TLR5 and TLR9 but not TLR4, TLR6, TLR7, TLR8 or TLR10. It is well known that the so-called CpG motifs in bacterial DNA, such as pDNA, are recognized by TLR9 and trigger signaling pathways that activate various transcription factors, including NF- κ B and activator protein-1. These results suggest that the production of TNF- α might be due to CpG motif recognition by TLR9 expressed by KC. Polyplex formation would enhance cellular uptake of pDNA and its stability compared with naked pDNA. This effect would not be specific to mBSA, the cationic carrier used in this study, because the production of TNF- α from

KC was also detected when we use other cationic macromolecules, such as poly L-lysine (data not shown), to prepare the polyplex in our preliminary study.

Endogenous and exogenous antigens in DC followed by processing to antigen peptide are present on MHC class I and II molecule, respectively. The presentation of antigen peptide on MHC class II leads to antibody production following proliferation of CD4⁺ helper T cells. We believe that enhanced antibody production by polyplex-based DNA vaccination might be due, at least in part, to increased direct delivery of pDNA to DC in the treated skin. After endogenous antigen is expressed and secreted from DC, the DC itself or surrounding DC would be taken up by the antigen in the injection site and presented to MHC class II. It is also known that the endogenous antigen is also directly delivered via the MHC class II-restricted pathway in the cells [30–35].

It has been reported that the routes and methods of pDNA delivery affect the immunological consequences following DNA vaccination [36–38]. For example, intradermal administration has been shown to be more efficient than intramuscular administration as far as the induction of humoral immune response is concerned. pDNA delivered to the skin by intradermal injection or gene gun appears to activate the Th2 polarized response, whereas intramuscular injection of pDNA predominantly induces the Th1 response. The selection of pDNA formulations is also one of the most important factors for the determination of immune responses. It has been reported that adjuvants and delivery systems, such as cationic macroparticles [39,40], chitosan (in a case of mucosal vaccination) [41,42] and lipid vesicles [43,44], can be used not only to increase the strength of the immune response, but also to influence the types of induced cellular and antibody responses. Manipulation of DC migration using various chemokines, such as MIP-1 α , regulated on activation normal T cell expressed and secreted (RANTES) is also a promising approach [45,46]. The present study has demonstrated that polyplex-based DNA vaccination is another option for manipulating antigen-specific immune responses.

In conclusion, we have demonstrated that the immune responses can be biased towards the antibody production by polyplex-based DNA vaccination through manipulation of not only pDNA disposition and expression but also dendritic cell migration. We also considered that the inducibility for Th-2 type response is the advantage of polyplex-based DNA vaccination.

Acknowledgements

This work was supported in part by a Grant-in-Aid for Scientific Research from the Ministry of Education, Culture, Sports, Science and Technology of Japan, by Uehara Memorial Foundation and 21st Century COE Program “Knowledge Information Infrastructure for Genome Science”.

References

- [1] Tang DC, DeVit M, Johnston SA. Genetic immunization is a simple method for eliciting an immune response. *Nature* 1992;356(6365):152–4.
- [2] Ulmer JB, Donnelly JJ, Parker SE, Rhodes GH, Felgner PL, Dworki VJ, et al. Heterologous protection against influenza by injection of DNA encoding a viral protein. *Science* 1993;259(5102):1745–9.
- [3] Porgador A, Irvine KR, Iwasaki A, Barber BH, Restifo NP, Germain RN. Predominant role for directly transfected dendritic cells in antigen presentation to CD8⁺ T cells after gene gun immunization. *J Exp Med* 1998;188(6):1075–82.
- [4] Shedlock DJ, Weiner DB. DNA vaccination: antigen presentation and the induction of immunity. *J Leukoc Biol* 2000;68(6):793–806.
- [5] Maecker HT, Umetsu DT, DeKruyff RH, Levy S. DNA vaccination with cytokine fusion constructs biases the immune response to ovalbumin. *Vaccine* 1997;15(15):1687–96.
- [6] Gilkeson GS, Phippen AM, Pisetsky DS. Induction of cross-reactive anti-dsDNA antibodies in preautoimmune NZB/NZW mice by immunization with bacterial DNA. *J Clin Invest* 1995;95(3):1398–402.
- [7] Gilkeson GS, Ruiz P, Phippen AM, Alexander AL, Lefkowitz JB, Pisetsky DS. Modulation of renal disease in autoimmune NZB/NZW mice by immunization with bacterial DNA. *J Exp Med* 1996;183(4):1389–97.
- [8] Uchi H, Terao H, Koga T, Furue M. Cytokines and chemokines in the epidermis. *J Dermatol Sci* 2000;24(Suppl. 1):S29–38.
- [9] Wang B, Amerio P, Sauder DN. Role of cytokines in epidermal Langerhans cell migration. *J Leukoc Biol* 1999;66(1):33–9.
- [10] Cumberbatch M, Dearman RJ, Kimber I. Langerhans cells require signals from both tumour necrosis factor- α and interleukin-1 β for migration. *Immunology* 1997;92(3):388–95.
- [11] Cotten M, Baker A, Saltik M, Wagner E, Buschle M. Lipopolysaccharide is a frequent contaminant of plasmid DNA preparations and can be toxic to primary human cells in the presence of adenovirus. *Gene Ther* 1994;1(4):239–46.
- [12] Hartmann G, Krieg AM. CpG DNA and LPS induce distinct patterns of activation in human monocytes. *Gene Ther* 1999;6(5):893–903.
- [13] Mandell JD, Hershey AD. A fractionating column for analysis of nucleic acids. *Anal Biochem* 1960;1:66–77.
- [14] Chonn A, Semple SC, Cullis PR. Association of blood proteins with large unilamellar liposomes in vivo. Relation to circulation lifetimes. *J Biol Chem* 1992;267(26):18759–65.
- [15] Ito D, Ogasawara K, Iwabuchi K, Inuyama Y, Onoe K. Induction of CTL responses by simultaneous administration of liposomal peptide vaccine with anti-CD40 and anti-CTLA-4 mAb. *J Immunol* 2000;164(3):1230–5.
- [16] McNeela EA, Mills KH. Manipulating the immune system: humoral versus cell-mediated immunity. *Adv Drug Deliv Rev* 2001; 51(1–3):43–54.
- [17] Donnelly JJ, Ulmer JB, Shiver JW, Liu MA. DNA vaccines. *Annu Rev Immunol* 1997;15:617–48.
- [18] Howard KA, Alpar HO. The development of polyplex-based DNA vaccines. *J Drug Target* 2002;10(2):143–51.
- [19] Howard KA, Li XW, Somavarapu S, Singh J, Green N, Atuah KN, et al. Formulation of a microparticle carrier for oral polyplex-based DNA vaccines. *Biochim Biophys Acta* 2004;1674(2):149–57.
- [20] Schlecht G, Leclerc C, Dadaglio G. Induction of CTL and nonpolarized Th cell responses by CD8 α (+) and CD8 α (-) dendritic cells. *J Immunol* 2001;167(8):4215–21, 15.
- [21] Kawase A, Kobayashi N, Isaji K, Nishikawa M, Takakura Y. Manipulation of local disposition and gene expression characteristics of plasmid DNA following intramuscular administration by complexation with cationic macromolecule. *Int J Pharm* 2005;293(1–2):291–301, 11.
- [22] Coyle AJ, Perretti F, Manzini S, Irvin CG. Cationic protein-induced sensory nerve activation: role of substance P in airway

- hyperresponsiveness and plasma protein extravasation. *J Clin Invest* 1994;94(6):2301–6.
- [23] Okayama Y, el-Lati SG, Leiferman KM, Church MK. Eosinophil granule proteins inhibit substance P-induced histamine release from human skin mast cells. *J Allergy Clin Immunol* 1994;93(5):900–9.
- [24] Manske JM, Hanson SE. Substance-P-mediated immunomodulation of tumor growth in a murine model. *Neuroimmunomodulation* 2005;12(4):201–10.
- [25] Tohyama M, Shirakara Y, Yamasaki K, Sayama K, Hashimoto K. Differentiated keratinocytes are responsible for TNF-alpha regulated production of macrophage inflammatory protein 3alpha/CCL20, a potent chemokine for Langerhans cells. *J Dermatol Sci* 2001;27(2):130–9.
- [26] Dieu-Nosjean MC, Massacrier C, Homey B, Vanbervliet B, Pin JJ, Vicari A, et al. Macrophage inflammatory protein 3alpha is expressed at inflamed epithelial surfaces and is the most potent chemokine known in attracting Langerhans cell precursors. *J Exp Med* 2000;192(5):705–18.
- [27] Mempel M, Voelcker V, Kollisch G, Plank C, Rad R, Gerhard M, et al. Toll-like receptor expression in human keratinocytes: nuclear factor kappaB controlled gene activation by *Staphylococcus aureus* is toll-like receptor 2 but not toll-like receptor 4 or platelet activating factor receptor dependent. *J Invest Dermatol* 2003;121(6):1389–96.
- [28] Krieg AM. CpG motifs in bacterial DNA and their immune effects. *Annu Rev Immunol* 2002;20:709–60.
- [29] Zhao Q, Tamsamani J, Zhou RZ, Agrawal S. Pattern and kinetics of cytokine production following administration of phosphorothioate oligonucleotides in mice. *Antisense Nucleic Acid Drug Dev* 1997;7(5):495–502.
- [30] Nuchtern JG, Biddison WE, Klausner RD. Class II MHC molecules can use the endogenous pathway of antigen presentation. *Nature* 1990;343(6253):74–6.
- [31] Sant AJ. Endogenous antigen presentation by MHC class II molecules. *Immunol Res* 1994;13(4):253–67.
- [32] Oxenius AM, Bachmann F, Ashton-Rickardt PG, Tonegawa S, Zinkernagel RM, Hengartner H. Presentation of endogenous viral proteins in association with major histocompatibility complex class II: on the role of intracellular compartmentalization, invariant chain and the TAP transporter system. *Eur J Immunol* 1995;25(12):3402–11.
- [33] Lechler R, Aichinger G, Lightstone L. The endogenous pathway of MHC class II antigen presentation. *Immunol Rev* 1996;151:51–79.
- [34] Koch N, van Driel IR, Gleeson PA. Hijacking a chaperone: manipulation of the MHC class II presentation pathway. *Immunol Today* 2000;21(11):546–50.
- [35] Qi L, Ostrand-Rosenberg S. MHC class II presentation of endogenous tumor antigen by cellular vaccines depends on the endocytic pathway but not H2-M. *Traffic* 2000;1(2):152–60.
- [36] Pertmer TM, Roberts TR, Haynes JR. Influenza virus nucleoprotein-specific immunoglobulin G subclass and cytokine responses elicited by DNA vaccination are dependent on the route of vector DNA delivery. *J Virol* 1996;70(9):6119–25.
- [37] Feltquate DM, Heaney S, Webster RG, Robinson HL. Different T helper cell types and antibody isotypes generated by saline and gene gun DNA immunization. *J Immunol* 1997;158(5):2278–84.
- [38] Yoshida A, Nagata T, Uchijima M, Higashi T, Koide Y. Advantage of gene gun-mediated over intramuscular inoculation of plasmid DNA vaccine in reproducible induction of specific immune responses. *Vaccine* 2000;18(17):1725–9.
- [39] Singh M, Briones M, Ott G, O'Hagan D. Cationic microparticles: A potent delivery system for DNA vaccines. *Proc Natl Acad Sci USA* 2000;97(2):811–6.
- [40] Denis-Mize KS, Dupuis M, MacKichan ML, Singh M, Doe B, O'Hagan D, et al. Plasmid DNA adsorbed onto cationic microparticles mediates target gene expression and antigen presentation by dendritic cells. *Gene Ther* 2000;7(24):2105–12.
- [41] McNeela EA, O'Connor D, Jabbal-Gill I, Illum L, Davis SS, Pizzia M, et al. A mucosal vaccine against diphtheria: formulation of cross reacting material (CRM(197)) of diphtheria toxin with chitosan enhances local and systemic antibody and Th2 responses following nasal delivery. *Vaccine* 2000;19(9–10):1188–98.
- [42] Jabbal-Gill I, Fisher AN, Rappuoli R, Davis SS, Illum L. Stimulation of mucosal and systemic antibody responses against *Bordetella pertussis* filamentous haemagglutinin and recombinant pertussis toxin after nasal administration with chitosan in mice. *Vaccine* 1998;16(20):2039–46.
- [43] Bramwell VW, Eyles JE, Somavarapu S, Alpar HO. Liposome/DNA complexes coated with biodegradable PLA improve immune responses to plasmid encoding hepatitis B surface antigen. *Immunology* 2002;106(3):412–8.
- [44] Klavinskis LS, Gao L, Barnfield C, Lehner T, Parker S. Mucosal immunization with DNA-liposome complexes. *Vaccine* 1997;15(8):818–20.
- [45] Yamazaki S, Yokozeki H, Satoh T, Katayama I, Nishioka K. TNF-alpha, RANTES, and MCP-1 are major chemoattractants of murine Langerhans cells to the regional lymph nodes. *Exp Dermatol* 1998;7(1):35–41.
- [46] Sozzani S, Sallusto F, Luini W, Zhou D, Piemonti L, Allavena P, et al. Migration of dendritic cells in response to formyl peptides, C5a, and a distinct set of chemokines. *J Immunol* 1995;155(7):3292–5.

Analysis of In Vivo Nuclear Factor- κ B Activation during Liver Inflammation in Mice: Prevention by Catalase Delivery^S

Kenji Hyoudou, Makiya Nishikawa, Yuki Kobayashi, Yukari Kuramoto, Fumiyoshi Yamashita, and Mitsuru Hashida

Departments of Drug Delivery Research (K.H., Y.K., Y.K., F.Y., M.H.) and Biopharmaceutics and Drug Metabolism (M.N.), Graduate School of Pharmaceutical Sciences, Kyoto University, Kyoto, Japan

Received May 25, 2006; accepted November 14, 2006

ABSTRACT

Nuclear factor- κ B (NF- κ B) is a transcription factor that plays crucial roles in inflammation, immunity, cell proliferation, and apoptosis. Until now, there have been few studies of NF- κ B activation in whole animals because of experimental difficulties. Here, we show that mice receiving a simple injection of plasmid vectors can be used to examine NF- κ B activation in the liver. Two plasmid vectors, pNF- κ B-Luc (firefly luciferase gene) and pRL-SV40 (*Renilla reniformis luciferase* gene), were injected into the tail vein of mice by the hydrodynamics-based procedure, an established method of gene transfer to mouse liver. Then, the ratio of the firefly and *R. reniformis* luciferase activities (F/R) was used as an indicator of the NF- κ B activity in the liver. Injection of thioacetamide or lipopolysaccharide plus D-galactosamine increased the F/R ratio in the liver, and this was

significantly ($P < 0.001$) inhibited by an intravenous injection of catalase derivatives targeting liver nonparenchymal cells. Imaging the firefly luciferase expression in live mice clearly demonstrated that the catalase derivatives efficiently prevented the NF- κ B-mediated expression of the firefly luciferase gene. Plasma transaminases and the survival rate of mice supported the findings obtained by the luminescence-based analyses. Thus, this method, which requires no genetic recombination techniques, is highly sensitive to the activation of NF- κ B and allows us to continuously examine the activation in live animals. In conclusion, this novel, simple, and sensitive method can be used not only for analyzing the NF- κ B activation in the organ under different inflammatory conditions but also for screening drug candidates for the prevention of liver inflammation.

Liver inflammation is a highly important event occurring in various conditions including ischemia/reperfusion injury, viral infection, drug-induced hepatic injury, and septic shock (Loguercio and Federico, 2003). The inflammation is normally associated with the induction of inflammatory cytokines, such as tumor necrosis factor- α (TNF- α) and interferon- γ . Active transcription of these molecules leads to inflammatory damage to organs, in which activation of transcription factors takes place. Nuclear factor κ B (NF- κ B) is a transcription factor that plays crucial roles in inflammation,

immunity, cell proliferation, and apoptosis (Viatour et al., 2005). Activation of NF- κ B mainly occurs via I κ B kinase-mediated phosphorylation of inhibitory molecules, including I κ B α . Expression of NF- κ B-inducible genes also requires phosphorylation of NF- κ B proteins, such as p65, by a variety of kinases in response to distinct stimuli. Because deregulation of NF- κ B and I κ B phosphorylation is a hallmark of long-term inflammatory diseases and cancer, newly designed drugs targeting these constitutively activated-signaling pathways are promising therapeutic agents. However, to date, NF- κ B activation has not been properly investigated in whole animals because of experimental difficulties. Although antibodies and immunofluorescence assays of NF- κ B can be used in mechanistic studies of specific compounds to detect NF- κ B activation (van den Berg et al., 2001; Shen et al., 2002), these methods are cumbersome, complicated, and expensive. Therefore, a simple and reliable method to detect NF- κ B activation is useful for screening drug candidates. Here, we report that mice receiving a simple injection of

This work was supported in part by Grants-in-Aid for Scientific Research from the Ministry of Education, Culture, Sports, Science and Technology of Japan, by Health and Labor Sciences Research Grants for Research on Hepatitis and BSE from the Ministry of Health, Labor and Welfare of Japan and by the 21st Century COE Program "Knowledge Information Infrastructure for Genome Science."

Article, publication date, and citation information can be found at <http://molpharm.aspetjournals.org>.

doi:10.1124/mol.106.027169.

^S The online version of this article (available at <http://molpharm.aspetjournals.org>) contains supplemental material.

ABBREVIATIONS: TNF, tumor necrosis factor; Gal-catalase, galactosylated catalase; Man-catalase, mannosylated catalase; PEG-catalase, polyethyleneglycol-conjugated catalase; Suc-catalase, succinylated catalase; TA, thioacetamide; LPS, lipopolysaccharide; GalN, D-galactosamine; IL, interleukin; ROS, reactive oxygen species; EMSA, electrophoretic mobility shift assay; NF- κ B, nuclear factor- κ B; F/R, ratio of the firefly and *Renilla reniformis* luciferase activities; AST, aspartate aminotransferase; ALT, alanine aminotransferase; SV40, simian virus 40.

plasmid vectors can be used as a model to examine NF- κ B activity in the liver. Liver inflammation through NF- κ B activation is induced by intraperitoneal injection of thioacetamide (TA) or lipopolysaccharide (LPS) plus D-galactosamine (GalN) in mice, and the inhibitory effect of chemically modified catalase derivatives targeting liver nonparenchymal cells on the TA- or LPS/GalN-induced inflammation is demonstrated.

Materials and Methods

Animals. Male C57/BL6 (6-week-old) and BALB/c (5-week-old) mice were purchased from the Shizuoka Agricultural Cooperative Association for Laboratory Animals (Shizuoka, Japan). Animals were maintained under conventional housing conditions. All animal experiments were conducted in accordance with the principles and procedures outlined in the U.S. National Institutes of Health Guide for the Care and Use of Laboratory Animals. The protocols for animal experiments were approved by the Animal Experimentation Committee of the Graduate School of Pharmaceutical Sciences of Kyoto University. BALB/c mice were used for the imaging of luciferase expression to avoid light extinction, and C57/BL6 mice were used for the other experiments.

Chemicals. TA, LPS (from *Escherichia coli* 0111:B4), GalN, and bovine liver catalase (C-100, 40,000 U/mg) were purchased from Sigma Chemical (St. Louis, MO). D-Luciferin was purchased from Promega (Madison, WI). Galactosylated (Gal-), mannosylated (Man-), polyethyleneglycol-conjugated (PEG-), or succinylated (Suc-) catalase was synthesized, and its enzymatic activity was measured as reported previously (Yabe et al., 1999a). All other chemicals were of the highest grade commercially available.

Plasmid DNA. pNF- κ B-Luc encoding firefly luciferase gene driven by a basic promoter element plus five tandem copies of NF- κ B binding elements [(TGGGGACTTTCGCG)₅] was purchased from Stratagene (La Jolla, CA). pRL-SV40 encoding the *Renilla reniformis* luciferase gene under the control of SV40 promoter, which has no NF- κ B binding sequences, was purchased from Promega (Madison, WI). Plasmid DNA was injected into the tail vein of mice by the hydrodynamics-based procedure (Liu et al., 1999; Zhang et al., 1999; Kobayashi et al., 2001, 2002, 2004), which is an established method for in vivo gene transfer to the liver. According to previous reports, plasmid DNA dissolved in 1.5 ml of saline was injected into the tail vein within 5 s. Based on the sensitivity of the assays, the doses of plasmid DNA were set at 5 μ g/mouse for pNF- κ B-Luc for the in vivo imaging study and 0.1 μ g/mouse each for pNF κ B-Luc and pRL-SV40 for quantitative analysis.

Fulminant Liver Injury Model. TA (1000 mg/kg of body weight) or LPS (1 μ g/body) plus GalN (10 mg/body) were injected intraperitoneally into mice 24 h after the injection of plasmid DNA to induce a fulminant liver injury. The dose of TA or LPS/GalN was determined according to previous reports (Hwang et al., 2003; Okuyama et al., 2003). Saline (untreated, control group) or any catalase derivative was injected in the tail vein at a dose of 5000 catalase U/mouse just before TA or LPS/GalN injection. The dose of catalase was determined according to our previous studies, in which 100 to 10,000 units of catalase derivatives were administered in various experimental settings (Yabe et al., 1999a,b, 2001; Hyoudou et al., 2004; Ma et al., 2006). These studies and ones with other chemically modified proteins (Nishikawa et al., 1995; Opanasopit et al., 2001; Yamasaki et al., 2002) demonstrated that the delivery efficiency of chemically modified proteins will decrease with increasing dose. Therefore, any dose greater than the dose used (5000 U/mouse, which is equivalent to approximately 5 mg/kg of body weight) was not tested in the present study. In addition, this dose falls in the range of standard doses (<10 mg/kg of body weight) of protein drugs. At 24 h after TA or LPS/GalN injection, the luciferase activities in the liver were measured as described below. The survival of mice was also exam-

ined in a different set of mice treated in the same manner except for the hydrodynamic delivery of pDNA.

Luciferase Assay. At 24 h after TA or LPS/GalN injection, the liver was excised, homogenized, and centrifuged as reported previously (Hyoudou et al., 2004). Then, 10 μ l of the supernatant was mixed with 100 μ l of firefly luciferase assay buffer (Picagene, Toyo Ink, Tokyo, Japan) to detect firefly luciferase activity or 100 μ l *R. reniformis* luciferase assay buffer (Renilla Luciferase Assay System; Promega) to detect *R. reniformis* luciferase activity. The light produced was immediately measured using a luminometer (Lumat LB 9507; Berthold Technologies, Bad Wildbad, Germany). After subtraction of the background activity for the liver homogenate without injection, the ratio of the activity of the firefly luciferase to the *R. reniformis* luciferase was calculated to correct for differences in transfection efficiency among mice.

Luciferase Imaging. To avoid light extinction, white male BALB/c mice were used. At 24 h after TA or LPS/GalN injection, mice were injected intraperitoneally with 2 mg of D-luciferin, anesthetized with pentobarbital in phosphate-buffered saline, and then placed in a NightOwl LB 981 Molecular Light Imager (Berthold Technologies). Imaging was then performed in a two-step process using WinLight32 software. First, a black-and-white photographic image was acquired using a 15-ms exposure. Next, the luminescent image was acquired using a 5-min photon integration period with background subtraction. The luminescent image was processed by the software to color the luminescence intensity and then overlaid onto the photographic image. The parameters in the WinLight32 software used to obtain luminescent images were as follows: color threshold, 500 to 5000; color scheme, linear.

Determination of Plasma Transaminase Activities. At 24 h after TA or LPS/GalN injection, blood was collected from the vena cava using a heparinized syringe, and plasma was obtained by centrifugation. Alanine aminotransferase (ALT) and aspartate aminotransferase (AST) activities in the plasma were determined by commercially available test reagents (Transaminase test Wako; Wako, Osaka, Japan). Control values were determined using the blood obtained from age-matched, untreated mice.

Electrophoretic Mobility Shift Assay. At 12 h after TA or LPS/GalN injection, the liver was excised, and nuclear protein was extracted with a CellLytic Nuclear Extraction Kit (Sigma) according to the manufacturer's instructions. Then, the nuclear protein was adjusted to 5 μ g/ μ l with water, and electrophoretic mobility shift assay (EMSA) was performed with EMSA Gel-Shift Kits (Panomics, Redwood City, CA), which contains consensus NF- κ B binding oligonucleotide (AGTTGAGGGGACTTCCAGGC). Nuclear extracts from HeLa cells containing NF- κ B protein were mixed with the labeled and unlabeled probe to obtain the positive and negative controls, respectively, and these were also used in the assay. Electrophoresis was performed with 7.5% polyacrylamide gel (Daiichi Pure Chemicals Co., Ltd., Tokyo, Japan). NF- κ B-derived luminescent bands were detected by a cooled charge-coupled device camera (Light Capture AE-6962; Atto Corporation, Tokyo, Japan) according to the manufacturer's instructions. A quantitative densitometry analysis was performed by CS analyzer (Atto Corporation).

Statistical Analysis. Differences were statistically evaluated by one-way analysis of variance followed by the Student-Neumann-Keuls multiple comparison test and Kaplan-Meier analysis with a Wilcoxon test to determine survival, and the level of statistical significance was $P < 0.05$.

Results

Expression of Firefly and *R. reniformis* Luciferases After In Vivo Gene Transfer. The firefly luciferase and *R. reniformis* luciferase activities peaked at 8 h after injection and then decreased with time, but both luciferase activities were high enough to be detected even 72 h after injection.

Figure 1A shows the time course of the F/R ratio in the liver of mice that were injected with pNF- κ B-Luc and pRL-SV40. The F/R ratio decreased with time from 3 to 24 h after pDNA injection and then remained constant after 24 h.

Then, we investigated the effects of TA or LPS/GalN on the firefly luciferase activity (Fig. 1B). An intraperitoneal injection of TA or LPS/GalN at 24 h after pDNA injection significantly ($P < 0.05$) increased the F/R ratio from 0.14 ± 0.03 (the saline-treated group) to 0.88 ± 0.24 and 0.52 ± 0.19 in the TA-treated and the LPS/GalN-treated groups, respectively, at 24 h after TA or LPS/GalN injection. These results clearly demonstrated that NF- κ B is activated by TA or LPS/GalN. The *R. reniformis* luciferase activity in the TA-treated or the LPS/GalN-treated mice was not significantly different from that of saline-treated mice (data not shown).

Luminescence-Based Analysis of Thioacetamide-Induced NF- κ B Activation in Mouse Liver. Because ROS activates NF- κ B (Piette et al., 1997), we examined whether scavenging of ROS by catalase derivatives suppresses the expression of firefly luciferase gene in the present model. As shown in Fig. 2A, a large amount of firefly luciferase-derived luminescence was detected in the liver of the saline-treated live mice. The luminescence intensity was converted to a heat map image by WinLight32 software. An intravenous injection of native catalase, PEG-, or Gal-catalase (5000 U/mouse)

suppressed the expression to a degree. However, Man- or Suc-catalase, both of which are delivered to liver nonparenchymal cells (Yabe et al., 1999a), markedly reduced the luminescence in the liver. A quantitative luciferase assay gave results similar to those of the imaging study (Fig. 2B). Man- or Suc-catalase significantly ($P < 0.001$) reduced the F/R ratio in the liver, clearly demonstrating that the catalase derivatives targeting liver nonparenchymal cells efficiently prevent NF- κ B activation.

Effect of Catalase Derivatives on Thioacetamide-Induced Liver Injury. The hepatic enzymes, AST and ALT, are frequently used as indicators of liver damage. It has been reported that TA causes lethal liver damage with high serum AST and ALT activities (Diez-Fernandez et al., 1993). In the present model, a marked increase in AST and ALT levels was

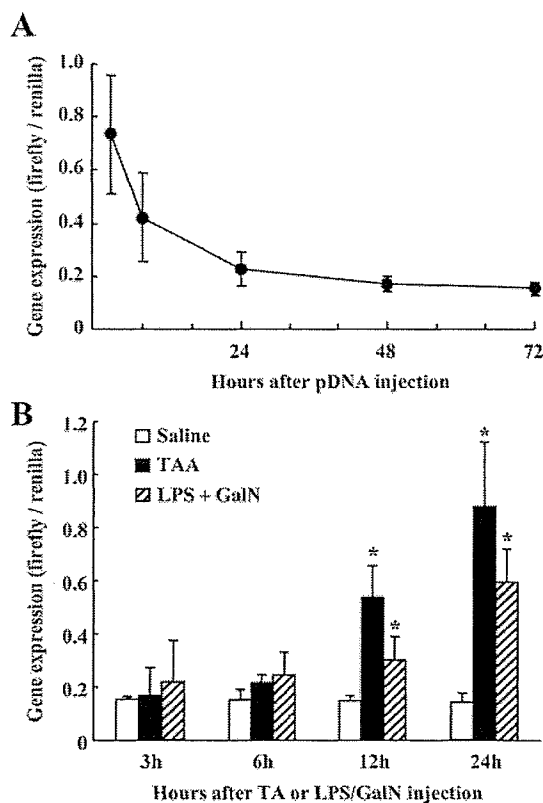


Fig. 1. The ratio of firefly and *R. reniformis* luciferases (F/R ratio) in the liver. A, mice were killed at 3, 8, 24, 48, or 72 h after pDNA injection, and the luciferase activity in the liver was assayed. Results are expressed as the mean \pm S.D. of at least three mice. B, effect of TA or LPS/GalN on the F/R ratio. TA or LPS/GalN was intraperitoneally injected 24 h after pDNA injection, and the luciferase activity in the liver was assayed 3, 6, 12, or 24 h after TA or LPS/GalN injection. Results are expressed as the mean \pm SD of at least three mice. *, a statistically significant difference compared with the saline-treated group ($P < 0.05$).

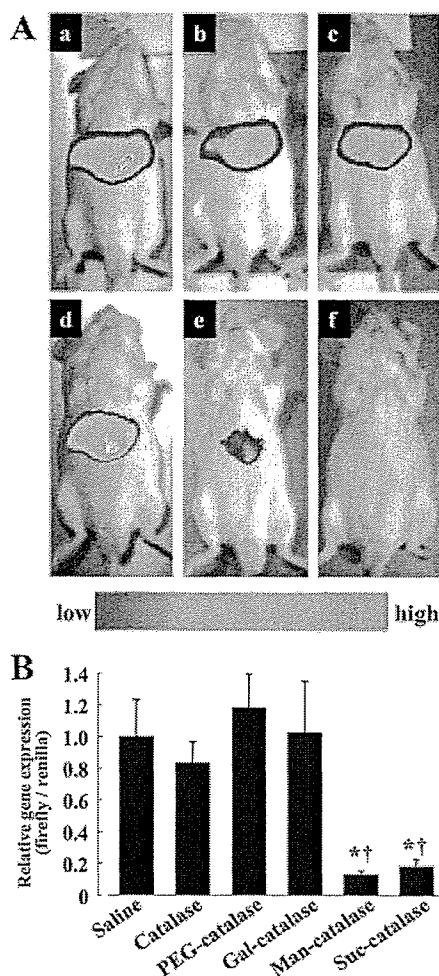


Fig. 2. Effect of catalase derivatives on the activation of NF- κ B. TA was intraperitoneally injected 24 h after pDNA injection. Saline (vehicle) or any catalase derivative (5000 units/mouse) was intravenously injected just before the TA injection. A, visualization of firefly luciferase gene expression in live mice 24 h after TA injection. a, saline; b, catalase; c, PEG-catalase; d, Gal-catalase; e, Man-catalase; f, Suc-catalase. The luminescent signals were color-coded based on the color scale below the images. B, mice were killed 24 h after TA injection, and the luciferase activities in the liver were assayed. Relative gene expression was indicated as an x -fold increase compared with the saline-treatment group. Results are expressed as the mean \pm SD of four mice. *, a statistically significant difference compared with the saline-treated group ($P < 0.001$); †, a statistically significant difference compared with the catalase-treated group ($P < 0.001$).